INVESTIGATING THE EFFECTS OF ENVIRONMENTAL FACTORS ON THE SPREAD OF ANTIBIOTIC RESISTANT BACTERIA IN A DAIRY FACILITY

A Dissertation

by

HYOUNGMOOK PAK

Submitted to the Graduate and Professional School of
Texas A&M University
in partial fulfillment of the requirements for the degree of

DOCTOR OF PHILOSOPHY

Chair of Committee,	Maria D. King
Committee Members,	Ronald Lacey
	Yassin Hassan
	Victor Ugaz
Head of Department,	Patricia Smith

May 2022

Major Subject: Biological and Agricultural Engineering

ABSTRACT

Widespread use and availability of antibiotics has led to infectious and pathogenic bacteria developing antibiotic resistance. Various environmental factors, such as temperature, relative humidity, and wind, can also induce stress in bacterial cells, activating antibiotic resistance mechanisms to increase their survivability against harsh and extreme conditions. These bacteria can survive for a longer time and travel further distances if they become airborne, which is the case in many livestock facilities. Despite the increasingly recognized role of the environment in spreading pathogens, the mechanisms underlying environmental effects on the transmission of airborne bioparticles including viruses, bacteria and fungi remain poorly understood. In this research, aerosol, manure, and lagoon samples were collected from multiple locations throughout an open stall dairy facility in summer, winter, and spring to estimate the microbiome richness, taxonomic diversity, and antibiotic resistance. Temperature, relative humidity, and air velocity measurements at each sampling location were also recorded to examine environmental effects. Computational fluid dynamics (CFD) was utilized to investigate air flow movements and patterns within and around the dairy facility. CFD simulation results were compared with experimental air velocity measurements to confirm and validate their accuracies. Among the aerosol samples from three different seasons, samples collected in winter had the highest number of sequenced denoised reads, but had the least bacterial diversity. Disk diffusion test against eight different antibiotics revealed that bacteria showed strongest resistance in the winter aerosol samples and weakest

resistance in spring aerosol samples. Air velocities obtained by CFD simulations using ANSYS closely matched with experimental measurements around the dairy barn, but were slightly off inside due to the lack of obstacles in the simulations. It was shown that in winter, there was a high turbulence in the western side of the barn where also the strongest antibiotic resistance was detected in aerosol samples. Antibiotic resistant bacteria were revealed to be transported with air flow from the dairy barn out into the environment. This research as able to demonstrate the correlation of environmental factors on the microbiome diversity and antibiotic resistance of bacteria samples collected in different seasons as well as show the CFD can be used to estimate and model the air flow around a dairy facility accurately.

DEDICATION

I would like to dedicate this dissertation to my fiancé, Eujeen Hwang, for being by my side throughout this whole journey from the very beginning. I would also like to dedicate this dissertation to my father, Woong Chul Pak, my mother, Young-ho Hwang, and my brother, Hyoungmin Pak, for raising me with love, patience, faith, and laughter to become who I am today

ACKNOWLEDGEMENTS

First of all, I would like to thank my committee chair, Dr. Maria King, for her encouragement, support, guidance, and care throughout my Master's and Ph.D. studies. I would also like to thank my committee members, Dr. Ronald Lacey, Dr. Yassin Hassan, and Dr. Victor Ugaz for their deep insights throughout the course of this research. A special thank goes to Dr. Barbara Jones for inviting and helping me sample at the dairy facility.

Many thanks go to colleagues, faculty, and staff members in the BAEN department for making my time at Texas A&M University a great experience. I would like to thank Dr. Zong Liu for providing great guidance and opportunities. I would especially like to thank our amazing Aerosol Technology Laboratory team for all their help and energy.

I would like to deeply thank everyone from Vision Mission Church for their selfless services, for helping me grow spiritually, and for being a family in Christ during my decade-long stay in College Station.

Finally, I thank my father, my mother, and my brother for continuously checking up on me and providing their unending support, encouragement, motivation, and prayers. I would like to thank Eujeen Hwang, my love across space and time, for her abundant blessings, love, patience, strength, and courage from the start of my PhD studies.

CONTRIBUTORS AND FUNDING SOURCES

This work was supported by the USDA National Institute of Food and Agriculture, Hatch Project TEX09746.

NOMENCLATURE

ARG	Antibiotic resistance gene
ARB	Antibiotic resistant bacteria
OTU	Operational taxonomy unit
ASV	Amplicon sequence variant
HVAC	Heating, ventilation, air conditioning
CFD	Computational fluid dynamics
RANS	Reynolds averaged Navier-Stokes
k	turbulent kinetic energy
ε	turbulent dissipation rate
WWC	Wetted Wall Cyclone
QIIME2	Quantitative Insights Into Microbial Ecology 2
DADA2	Divisive Amplicon Denoising Algorithm 2
H	Height of building
U_y	Velocity at height y
U_{ref}	Velocity at the reference height
y_{ref}	Reference height, 1.5 m
α	Power law exponent, 0.14
U_*	Friction velocity
K_v	von Karman's constant, 0.4
C_μ	Model constant, 0.09
z_0	Surface roughness length, 0.025 m

TABLE OF CONTENTS

Page

LIST OF FIGURES

Page

LIST OF TABLES

Page

1. INTRODUCTION

1.1. The discovery and mechanisms of antibiotics

Antibiotics are molecules, either extracted from natural products or artificially synthesized, that possess certain activities against bacteria to inhibit their growth or kill them. Although the term antibiotic is sometimes used interchangeably with antimicrobial, antibiotic more specifically targets bacteria while antimicrobial can act against other microorganisms as well, such as parasites, fungi, and viruses. The first antibiotic to be developed was a man-made, synthetic agent called salvarsan by Paul Ehrlich in 1910 that was used to treat syphilis. This drug was derived from a crystalline power known as atoxyl, or arsanilic acid, and was found to be effective against the disease-causing bacterium *Treponema pallidum* (Burke, 1925). Advancement in antibiotic was followed by the discovery of prontosil, a sulfonamide drug, by Gerhard Domagk in 1932 (Otten, 1986). Sulfonamides were and still is widely used in hospitals and clinics due to its broad capability to counteract different infectious diseases and bacteria. Another famous development of antibiotic was the discovery of penicillin by Alexander Fleming in 1928 and the successful isolation of the compound by Ernst Chain, Norman Heatley, and Howard Florey in 1939 (Abraham et al., 1941). This novel drug was then actively mass produced to save countless soldiers to combat infections during World War II. Since the 1940s, more and more antibiotics, such as streptomycin, tetracycline, chloramphenicol, and ciprofloxacin, were introduced to fight against various bacterial infections and diseases (Nicolaou and Rigol, 2018).

Different classes of antibiotics use various mechanisms of action to inactivate bacteria. Majority of antibiotics can be categorized by four principal modes of action that inhibit: (1) cell wall synthesis, (2) protein synthesis, (3) DNA synthesis, and (4) folic acid metabolism (Tenover, 2006). Bacterial cell walls are targeted by antibiotics containing a β-lactam ring in their structures that inhibit active sites of enzymes necessary for synthesizing the peptidoglycan layer. Some examples of these β-lactam antibiotics include ampicillin, cefoperazone, cephalothin, and imipenem (Williams, 1996). A different type of antibiotics, such as gentamycin and tetracycline, attach to either the 30S or 50S subunit of bacterial ribosomes to inactivate the protein synthesis pathway (Yoneyama and Katsumata, 2006). Bacterial DNA is replicated with the help of DNA gyrase and topoisomerase IV in nicking the double strand. These enzymes are another target for antibiotics to bind and stop the DNA replication process. Ciprofloxacin uses this mechanism to inhibit bacteria (Kapoor et al., 2017). One of the earliest antibiotics to be discovered, sulfonamides, inhibit folic acid metabolism, which in turn disrupts DNA synthesis. Sulfonamide drugs are often used in conjunction with trimethoprim to create a synergistic effect in inhibiting folic acid metabolism. Sulfamethoxazole-trimethoprim is an example of this combination of antibiotic (Eliopoulos and Huovinen, 2001).

1.2. Emergence and mechanisms of antibiotic resistance

However, successful discoveries and implementations of antibiotics were quickly followed by equally successful developments of antibiotic resistance in bacteria. Numerous antibiotics are developed from secondary metabolites naturally produced by

bacteria. As they are used to treat bacterial infections in human patients, those products are used to protect themselves or kill competing microorganisms in their environment (Hutchings et al., 2019). Bacteria that produce antibiotics have developed mechanisms to express antibiotic resistance mechanisms concurrently or in advance. They are also capable of communicating with antibiotic non-producing cells to signal the expression of antibiotic resistance (Mak et al., 2014).

Resistance to antibiotics can either be intrinsic in nature or be acquired by various means. An example of intrinsic resistance could be if the bacteria does not possess the specific target site for a selected antibiotic to bind to. Similar to antibiotics, antibiotic resistance also has several mechanisms of action that prevent them from inhibiting essential biochemical pathways in bacteria. These mechanisms, such as reduced permeability through cell membrane, increased antibiotics efflux, modified target sites, and inactivation of antibiotics, increase bacteria's survivability against broad classes of antibiotics (Blair et al., 2015). Reducing the permeability of antibiotics through the bacterial cell membrane can prevent certain antibiotics from entering the system. This first line of defense is achieved by down-regulating or replacing porin enzymes in the outer membrane (Tamber and Hancock, 2003). There are several substrate-specific efflux pumps that can pump out certain antibiotics and multidrug resistance efflux pumps that can transport multiple antibiotics out through the membrane (Uddin and Ahn, 2018). It was shown in a study that when linezolid, which targets the ribosomal subunit, was used on *Streptococcus pneumoniae,* mutations occurred in the gene that encodes the ribosome, preventing the binding of the antibiotic to the modified target site (Billal et al., 2011).

Another mechanism in which bacteria gain antibiotic resistance is to produce enzymes that can hydrolyze specific antibiotics. A well-known example is β-lactamases that can degrade β-lactam antibiotics (Ghafourian et al., 2015).

Adverse environmental conditions and stresses can also induce adaptive responses similar to antibiotic resistance in bacteria to increase their survivability and spread such mechanisms. When the integrity of bacterial cell envelope is threatened by external factors, bacteria activates response certain mechanisms, such as membrane modification and inducing efflux systems, which are similar to antibiotic resistance (Poole, 2012). Persisters, or dormant cells, also display accelerated antibiotic resistance by increasing the number of culturable cells and mutation rates (Windels et al., 2019). It was observed when *Pseudomonas aeruginosa* was exposed to heat shock treatments, there was an overexpression of aminoglycoside resistance, indicating that exposure to higher temperatures increases resistance against antibiotics (Kindrachuk et al., 2011). A similar trend was shown when *Listeria monocytogenes* was cold-stressed at 10 °C for 24 hours. The treated bacteria showed significantly increased resistance ($P < 0.05$) against nine different antibiotics. This resistance was still present even after the bacteria was incubated at 37 °C for 24 hours (Al-Nabulsi et al., 2015).

1.3. Spread of antibiotic resistance in the environment

Many of the above-mentioned mechanisms of resistance are encoded by antibiotic resistant genes (ARGs) located either in the bacterial DNA or plasmids. Surviving bacteria then passes on those ARGs through horizontal gene transfer, or conjugation. Although the

phenomena of gene transfer are extensively studied in laboratory settings, it is thought that sharing of ARGs occur much more frequently and abundantly in nature (Davies and Davies, 2010). Mobile genetic elements, such as transposons and integrons, are located either in plasmids or chromosomes and can "jump" around different locations in the bacterial DNA. Many transposons and integrons, such as the class 1 integron-integrase gene (intI1), are known to carry ARGs (Zheng et al., 2020). This enables recipient bacteria to acquire resistance against different antibiotics without ever having being exposed to them, leading to the emergence of superbugs, or multiple drug resistance microorganisms. Every year, it is reported that over 60,000 patients in United States and 25,000 patients in Europe die from bacterial infections caused by those antibiotic resistant bacteria (ARB). The decrease in effectiveness and development of antibiotics with the increase and spread of antibiotic resistance is shifting the world towards a post-antibiotic era (Zaman et al., 2017).

Resistance against antibiotics is a phenomenon not only observed in hospitals, but is also prevalent in the environment and other facilities (Edelsberg et al., 2014; Gao et al., 2018; Mirhoseini et al., 2016). Bacteria in the environment exposed to antibiotics and pharmaceutical ingredients near industrial effluents quickly develop antibiotic resistance due to selective pressure (Larsson, 2014). Due to overuse of antibiotics and disposal of unused antibiotics, wastewater and wastewater treatment facilities have shown increase in antibiotic resistant genes and bacteria, both in effluents and air (Hassoun-Kheir et al., 2020; Kumar and Pal, 2018). A study in an office workspace showed that bacteria in the air were pathogenic and resistant to multiple antibiotics (Brągoszewska and Biedroń,

2018). They can even interact with each other and form biofilms for additional protection and survival. Air samples collected from 174 automobile air conditioner filters around the world in 19 urban cities demonstrated the presence and abundance of multiple ARGs being transmitted through the air (Li et al., 2018). It has also been reported that ARGs against tetracycline and sulfonamide can naturally occur in soils without prior exposure to antibiotics. Antibiotic resistance was detected in soil samples from organic farms, where the use of antibiotics is restricted but animal manures are sometimes applied (Cadena et al., 2018).

Use of antibiotics and spread of antibiotic resistance are also prominent in livestock facilities. For the past several decades, antibiotics have been globally used in food production for growth promotion, therapeutic, and prophylactic reasons. Although many countries have been successful in reducing and banning the use of antibiotics in animal feeds, antibiotics have become deeply rooted into livestock production in other first world countries, despite continuous efforts and warnings by international governments and organizations (Kirchhelle, 2018). In 2019 alone, more than 11 million kg of medically important antibiotics were marketed in United States for food-producing animals, such as cattle (FDA, 2020). As a result, resistant genes against several antibiotics, such as ampicillin, tetracyclines, and sulfonamides, are found in surfaces, air, manure, and soil from different livestock facilities (Adams et al., 2018; Ling et al., 2013; Munir and Xagoraraki, 2011). These ARGs can then become airborne and transported via particulate matter (PM) and wind (McEachran et al., 2015). Accumulation and dispersion of ARGs

in livestock facilities to surrounding environment pose a critical threat to the health of both animals and people if not monitored properly.

1.4. Environmental effects on the dissemination and survivability of bacteria in bioaerosol

Bacteria resistant to antibiotics can become airborne and spread from livestock facility into the open environment in the form of bioaerosols. Bioaerosol, or biological aerosol, are airborne liquid droplets that contain viable microorganisms, such as bacteria, fungi, and viruses, or other particles, such as pollen, toxins, and dust (Cox and Wathes, 1995). The constituents and density of aerosolized ARB depends on the particle size and origin of bioaerosols. Aerosol droplets can be as large as 100 μm in diameter, but particle diameters below 10 μm are of interest because if inhaled, they can reach deep into the human respiratory tract and cause adverse health effects (Fernstrom and Goldblatt, 2013). The size and number of aerosolized particles can be used to calculate their concentration. Depending on where the bioaerosol were generated is also of concern in order to determine their level of danger. ARB can be suspended in the air by simple everyday human activities, such as sneezing and coughing, or by aeration systems in wastewater treatment facilities, raindrops, spraying, irrigation, evaporation, and composting (Mirskaya and Agranovski, 2018). Bioaerosol provides a protection layer around ARB, enabling them to survive for a longer time and travel great distances without drying out.

Different environmental factors, such as temperature and relative humidity, affect the viability of aerosolized bacteria. Researches have been conducted using various ranges

of temperature and relative humidity to determine the survivability of airborne bacteria (Hoeksma et al., 2015; Marthi et al., 1990; Tang, 2009). It has been shown that bacteria can survive in bioaerosol between 10 to 30 °C, but the survivability is shown to be decreasing above 24 °C. The effect of relative humidity on airborne bacteria was less predictable as bacteria showed variable death and survival rates in different ranges of humidity. One explanation for this could be that because relative humidity is a ratio of the amount of water vapor pressure in the air over the total water vapor pressure possible in saturated air at a given temperature (Zhao et al., 2012). This signifies that relative humidity is a dependent variable reliant on temperature.

1.5. Analyzing the microbiome diversity in environmental samples

Bacteria collected from environmental samples are too diverse in species and numerous that it requires powerful and efficient tools for detailed analysis. Sequencing method for DNA was first introduced by Frederick Sanger in 1977 using a chain termination method and gel electrophoresis to identify its nucleotide sequences (Sanger et al., 1977). This discovery revolutionized the field of genetics and the advancement of modern equipment and methods in DNA sequencing. This led to next generation sequencing technologies that significantly lowered the cost and time per sequencing (Mardis, 2008). There are different types of DNA sequencing, such as whole genome sequencing and targeted region sequencing, that can be tailored towards specific research interests.

Examining bacteria diversity in environmental samples can be challenging because not all bacteria are culturable in the lab, meaning that although they may still be viable, they cannot grow on growth media (Oliver, 2005). In this case, 16S rRNA sequencing is well-known and commonly utilized procedure that can be used to overcome this challenge. One of the main advantages of using 16S rRNA gene, which is about 1,500 base pairs long, is that it is found in almost every bacterium (Janda and Abbott, 2007). It has nine variable regions surrounded by conservative regions that enable the classification of bacterial taxonomy (Claesson et al., 2010). In Illumina sequencing, DNA sequences are first fragmented into smaller sequences. Adapters are ligated to the ends of the DNA fragments and loaded onto a flow cell where they are amplified using the bridge amplification method. Then fluorescently-labeled dNTPs are attached to the DNA single strands emitting specific color lights. These images are automatically recorded to create sequence reads for all the DNA fragments. The reads are compiled together and are aligned with a reference genome to identify which taxonomy they belong (Illumina, 2017).

Sequenced reads can be further analyzed using an open-source pipeline called QIIME2 (pronounced “chime 2”), which stands for Quantitative Insights Into Microbial Ecology (Caporaso et al., 2010). This tool incorporates various tools interpret raw sequence data from assigning operational taxonomic units (OTUs), denoising sequences, aligning reads, building phylogenetic trees, arranging taxonomy, and comparing diversities (Hall and Beiko, 2018). Once the reads are imported into the QIIME2 environment, sequences that are usually 97% similar to each other are clustered into the same OTU using DADA2 (Divisive Amplicon Denoising Algorithm 2) (Callahan et al.,

2016). A more accurate form of distinguishing errors between sequences was developed to assign amplicon sequence variants (ASVs), which can detect sequence differences by one nucleotide (Callahan et al., 2017). A machine learning Python module is used in conjunction with a pre-trained naïve Bayes classifier re-trained against the SILVA database to classify taxonomies down to the species level (Pedregosa et al., 2011; Pruesse et al., 2007). Phylogenetic trees are generated using MAFFT and FastTree in QIIME2 to create a diversity metric between reads (Katoh and Standley, 2013; Price et al., 2010).

Similarities and differences between bacterial species in a sample can be compared using alpha and beta diversity measures. Alpha diversity illustrates the microbiome diversity within a sample while beta diversity shows similarities or dissimilarities of two environments (Whittaker, 1960). QIIME2 generates several metrics for alpha diversity, such as Faith's phylogenetic diversity and Shannon index, and beta diversity, such as UniFrac and Bray-Curtis (Bray and Curtis, 1957; Faith, 1992; Hall and Beiko, 2018; Lozupone and Knight, 2005; Shannon, 1948). In alpha diversity, richness – number of different species – and diversity – evenness or proportion of each species – are taken into account while beta diversity compares only diversity, or abundance, between samples (Konopiński, 2020). Alpha rarefaction curve indicates whether sufficient number of reads within a sample were sequenced in order to capture the majority of species. It has been shown that around 5,000 denoised reads were sufficient to capture most of the taxonomic profile within a sample using alpha diversity (Lundin et al., 2012). These methods provide a detailed overview of the diverse bacterial taxonomy present in environmental samples.

1.6. Computational fluid dynamics modelling in predicting air flow and aerosol dissemination

Bacteria enclosed in bioaerosols are also exposed to turbulent air flow, whether it is mechanically generated by the heating, ventilation, and air conditioning (HVAC) systems or naturally generated by wind. Computational fluid dynamics (CFD) is a powerful tool that is used to simulate and analyze complex air flow behavior. The rapid advancement and ease of accessibility to CFD tools enabled the performance of numerous complex simulations to investigate multiple variables, such as ventilation and heat transfer, in buildings (Wang and Zhai, 2016). In order to accurately portray the turbulent or laminar movement of fluid dynamics, certain processes, such as mesh generation, grid convergence, viscous turbulence model, boundary conditions, and numerical schemes, must be carefully and thoroughly planned out in the CFD simulations (Wang et al., 2018).

There are several governing equations that drive CFD simulations. Probably the most important equations that derives all other equations are the Navier-Stokes equations on the conservation of mass and momentum. These equations can be further solved three different techniques: direct numerical simulation (DNS), large eddy simulation (LES), and Reynolds averaged Navier-Stokes (RANS) (Joshi et al., 2011). This research will be focusing on the RANS method because DNS and LES approaches require too much computational time and power. The

In RANS, equations of mass and momentum conservation for incompressible flow, where density is constant, can be written as follows (Jehad et al., 2015):

$$\frac{\partial U_i}{\partial x_i} = 0 \tag{1}$$

$$U_j \frac{\partial U_i}{\partial x_j} = -\frac{1}{\rho}\frac{\partial p}{\partial x_i} + \frac{\partial}{\partial x_j}\left(\nu\left(\frac{\partial U_i}{\partial x_j} + \frac{\partial U_j}{\partial x_j}\right) - \overline{u_i' u_j'}\right) \tag{2}$$

where the Reynolds stresses ($\overline{u_i' u_j'}$) are solved using turbulence models. Two most commonly used turbulence models are two-equation models – k-ε and k-ω – that solve for turbulent kinetic energy (k) and dissipation rate (ε) or specific dissipation rate (ω). The standard k-ε model is widely used as it can accurately and robustly predict indoor air flow simulations using the following equations (Launder and Spalding, 1983):

$$U_i \frac{\partial k}{\partial x_i} - \frac{\partial}{\partial x_i}\left(\frac{\nu_T}{\sigma_k}\frac{\partial k}{\partial x_i}\right) = P - \varepsilon \tag{3}$$

$$U_j \frac{\partial \varepsilon}{\partial x_j} - \frac{\partial}{\partial x_i}\left(\frac{\nu_T}{\sigma_\varepsilon}\frac{\partial \varepsilon}{\partial x_i}\right) = \frac{\varepsilon}{k}(C_{\varepsilon 1} P - C_{\varepsilon 2}\varepsilon) \tag{4}$$

$$\nu_T = C_\mu \frac{k^2}{\varepsilon} \tag{5}$$

$$P_k = -\overline{u_i' u_j'}\left(\frac{\partial U_j}{\partial x_i} + \frac{\partial U_i}{\partial x_j}\right) \tag{6}$$

$$-\overline{u_i' u_j'} = \frac{2}{3}\delta_{ij} k + \nu_T\left(\frac{\partial U_j}{\partial x_i} + \frac{\partial U_i}{\partial x_j}\right) \tag{7}$$

where C_μ is 0.09, $C_{\varepsilon 1}$ is 1.44, $C_{\varepsilon 2}$ is 1.92, σ_k is 1.0, and σ_ε is 1.3. Another k-ε turbulence model called realizable k-ε model can better predict swirls and turbulence than

the standard model (Shih et al., 1995). The equations are same as the standard k-ε model, but the ε component is modified to:

$$\frac{\partial U_j \varepsilon}{\partial x_j} = \left(\mu + \frac{\mu_t}{\sigma_\varepsilon}\right)\nabla^2\varepsilon + C_1 S\rho\varepsilon - C_2\frac{\rho\varepsilon^2}{k+\sqrt{\upsilon\varepsilon}} \quad (8)$$

where $C_1 = max\left[0.43, \frac{\eta}{(\eta+5)}\right]$, $\eta = \frac{Sk}{\varepsilon}$, $S = \sqrt{2S_{ij}S_{ij,}}$ C_2 is 1.0, σ_k is 1.0, and σ_ε is 1.2. For k-ω turbulence, a shear stress transport (SST) k-ω model is commonly used as it is shown to perform better than the standard k-ε model, providing better accuracy and stability in turbulent flows around the walls and corners (Menter, 1993). Different turbulence models have their strengths and weaknesses, so they must be taken into consideration when using for CFD simulation and analysis (Zhai et al., 2007).

As mentioned before, CFD is used widely to examine air flow patterns and aerosol movement in various buildings. Studies have been conducted using CFD to investigate the effects of natural ventilation on a poultry house (Rojano et al., 2019), wastewater treatment plant (Maïzi et al., 2010), and dairy barns (Tomasello et al., 2019; Wu et al., 2012). A combination of natural and mechanical ventilation in dairy barns have been investigated (Pakari and Ghani, 2021). A much larger scale simulation is also possible to predict air flow over urban downtown (Ramirez et al., 2018). However, simulation results must always be validated with experimental measurements to provide an accurate understanding of fluid flow. In most cases, the variables of interest, such as air velocity, temperature, relative humidity, odor, particle size, or chemical concentration, are

measured and recorded on site. There are other scenarios where a scaled-down 3D model of the building is placed in a wind tunnel to simulate air flow to better visualize and measure the desired variables (Fossum et al., 2012; Saha et al., 2020). Numerous researches demonstrate that CFD simulations can accurately predict air flow patterns to monitor how bioaerosol are dispersed in buildings and their surrounding environment.

2. RESEARCH OBJECTIVES AND HYPOTHESIS

2.1. Research objective

With the widespread use and availability of antibiotics, more and more infectious and pathogenic bacteria have developed resistance to increase their chances of survival and reproduction. More exposure to antibiotics hastens the development and spread of antibiotic resistant bacteria (Alanis, 2005). Bacteria can transfer genes that encode resistance mechanisms against certain antibiotics to other species of bacteria via horizontal gene transfer. This is causing superbugs and multi-drug resistant bacteria to emerge, making it harder to treat bacterial diseases and hindering the production of new antibiotics. This is especially true in many livestock facilities where numerous antibiotics are used for medical purposes (Adams et al., 2018; Kirchhelle, 2018; Ling et al., 2013). The overuse of antibiotics and accumulation of manure in livestock facilities can create severe health risks for both the animals and humans. There are several researches on how different environmental factors, such as temperature, relative humidity, and wind, affect the survivability of bacteria in the atmosphere (Li et al., 2018; Nguyen et al., 2020; Wu et al., 2019). Computational fluid dynamics simulations are incorporated into many studies on livestock buildings to understand and predict how air flow patterns behave according to both natural and mechanical ventilations systems (Pakari and Ghani, 2021; Rojano et al., 2019; Saha et al., 2020; Tomasello et al., 2019; Wu et al., 2012). However, the effects of these variables on the development and dissemination of antibiotic resistance in bacteria are not clearly understood.

It is hypothesized that ARGs are not only triggered by the use and exposure of antibiotics, but also by different environmental factors, such as temperature, relative humidity, and wind. These variables could cause stress to develop in bacterial cells, triggering certain genes related to antibiotic resistance to increase their survivability against harsh and extreme conditions. Intensive research has been performed to understand the effects of environmental factors on the survivability of bacteria or inactivation of ARGs in aerosols and livestock manure, but it is not clear how antibiotic resistance is triggered and developed in bacteria under different stresses (Asheshov, 1966; Diehl and LaPara, 2010; Li et al., 2020b; Lin et al., 2017; MacFadden et al., 2018; Sun et al., 2016; Zhang et al., 2015). To prevent the spread of antibiotic resistant bacteria, it is crucial to gain a better understanding on how antibiotic resistance is activated in various environmental conditions.

Therefore, the objective of this research is to investigate how different environmental factors affect the development of antibiotic resistance in bacteria. To investigate, this study will be conducted in three steps. First, the bacterial microbiome richness and diversity in bioaerosol, manure, and lagoon samples collected from a dairy barn will be investigated and compared to different environmental samples, such as temperature and relative humidity, across three different seasons – summer, winter, and spring. Second, antibiotic resistance patterns in aerosol and manure samples from the three seasons will be investigated using the Kirby-Bauer disk diffusion method. Finally, CFD will be used to model and simulate air flow patterns in the dairy facility to analyze hotspots with high concentrations of bacteria exhibiting antibiotic resistance.

2.2. Research objective 1. Investigate environmental effects on bacteria diversity in a dairy facility in three seasons

2.2.1. Task 1. Collect bioaerosols, manure, lagoon water, and lagoon air from various locations in a dairy facility and record temperature, relative humidity, and air velocity measurements on the days of sampling.

Sampling will be conducted in a dairy facility in Stephenville in different seasons to collect bioaerosols, manure, and lagoon samples. The facility holds about 400 cows that are milked 3 times a day. There are 36 axial fans with water sprayers mounted on poles for evaporative cooling. Fans are all facing the northern side of the facility. Floors are periodically flooded with lagoon water from the northern side to the southern side to sweep out manure. Wetted Wall Cyclone (WWC) bioaerosol collectors will be used to collect aerosols by atomizing small amounts of collection liquid (milli-Q water) into the inlet section using an air blast atomizer (McFarland et al., 2010). The cyclones will collect air samples in various locations for 15 minutes at 100 L/min. Weather and environmental conditions, such as temperature, relative humidity, and wind speed, on the days of sampling will be monitored and recorded. The number of operational axial fans and their airflow speed and direction will also be recorded.

2.2.2. Task 2. Perform microbiome analysis on extracted bacterial DNA to determine genus and species of aerosolized bacteria

Bacterial DNA from the isolated colonies will be extracted using the alkaline lysis method (Zhou et al., 1990). The extracted DNA will be sent to the Texas A&M Institute for Genome Sciences and Society (TIGSS) for 16S rRNA Illumina sequencing using the Swift library preparation kit to obtain its microbiome data. The obtained sequences will be analyzed using QIIME2, naive Bayesian classifier, and SILVA database to identify the taxonomy of airborne bacteria. This information will be utilized to examine hotspots of antibiotic resistance and most frequently found genus and species of bacteria. Microbiome data from the two sampling periods will be compared to examine how different seasonal and environmental variables are correlated with different airborne bacteria species and antibiotic resistance.

2.3. Research Objective 2. Examine factors triggering antibiotic resistance in aerosol, manure, and water samples.

2.3.1. Task 1. Perform KB tests on bacteria isolates from bioaerosol and manure samples to examine their resistance against various antibiotics.

Collected samples will be plated on the same day of collection on TSA (Tryptic Soy Agar, Becton Dickinson) plates to obtain total culturable counts and colony forming units (CFUs). Kirby-Bauer disk diffusion test will be performed on isolated bacterial colonies to determine their level of resistance to eight different antibiotics. The zones of inhibition will be measured and compared with the antimicrobial susceptibility testing

standards from the Clinical and Laboratory Standards Institute to determine the level of resistance against antibiotics.

2.3.2. Task 2. Compare environmental factors in each sampling seasons to identify how they affect antibiotic resistance.

Environmental conditions, such as temperature, relative humidity, and wind velocities are expected to be different during different sampling trips. These will be recorded in each sampling location during collection periods using a HOBO data logger and hot-wire anemometer. Meteorological data for the collection day will also obtained from the weather station located in the dairy facility. Antibiotic resistance mapping obtained using KB tests will be compared with weather and environmental measurements across different seasons to investigate how they are related.

2.4. Research Objective 3. Model the movement of antibiotic resistant bacteria in dairy facility using computational fluid dynamics

2.4.1. Develop a 3D computational fluid dynamic model of the dairy facility.

The mechanical blueprint of the dairy facility layout will be used to design a 3D model and calculate air flow simulations. First, a simple model of the dairy facility will be created in SolidWorks and then imported in the ANSYS Fluent to investigate the air flow patterns from the open environment wind and from the axial fans. For simplification and reducing the computational power and load, obstacles within the dairy barn, such as fences, poles, and water troughs, will be removed. The CFD simulations will enable the

prediction of how air flow behaves around and within the open dairy barn. Cows will added to the model in a simplified form using a cylindrical configuration of their body or a porous media assumption (R. Mondaca and Y. Choi, 2016). The heat emission from each cow will also be considered in the simulation (Beck et al., 2019; Li et al., 2021).

Air flow simulations of the dairy facility model will be performed using ANSYS Fluent. Appropriate inlet, outlet, and wall parameters will be assigned in the mesh design regarding air velocity, pressure, and heat transfer. Boundary conditions will be set using the realizable k-ε turbulence model with enhanced wall treatment to perform a realistic and accurate CFD simulation and analysis. Turbulent properties will be calculated from the collected data points to investigate the how aerosolization and airflow patterns affect the development of antibiotic resistance in bacteria. Grid convergence index (GCI) will be calculated to validate that the uncertainties and errors in the fluid equations are accurately depicted. Particle tracking can be performed in ANSYS Fluent to investigate a more accurate simulation of different particle sizes and how they behave under the summer and winter air flow conditions.

2.4.2. Compare and validate model with experimental results (air velocities, microbiome analysis).

Hot-wire anemometers will be utilized to record air velocity measurements at the 15 locations where aerosol samples are collected to verify and validate the CFD simulation results. The temperature and relative humidity measurements taken with the HOBO data loggers will be included in the model. Weather data from the days of sample collection

will be obtained to examine how environmental wind along with the air movement from the 36 axial fans affect the air flow within the dairy facility.

3. METHODOLOGY

3.1. Sampling location

Three sampling campaigns in different seasons – Summer 2019, Winter 2020, Spring 2021 – were taken to an open-stall dairy farm in Texas to collect manure and aerosol samples. An aerial view of the dairy farm is shown in Figure 3.1A. There were 9 rows of 4 axial fans (J&D Manufacturing, Eau Claire, WI) – a total of 36 fans – located within the dairy facility moving air from the southern side to the northern side (Figure 3.1B). All fans were placed 4.5 m from the ground, tilted 15 degrees downwards, and operating at a velocity of 8.3 m/s. Water sprayers were attached to the fans to provide evaporative cooling for the cows. Fans were not operational in the winter as the temperature was cooler and there was no need for additional cooling of the cows. The facility held around 400 cows that were milked 3 times a day. When they were being milked, floors were flooded with lagoon water to wash off manure, which flowed down opposite to the direction of airflow. The accumulated water eventually flowed back into the lagoon and was reused for flooding. No antibiotics were incorporated into the feedstock. If cows became sick and had to take antibiotics, they were relocated to a nearby stall until antibiotics were removed from their system.

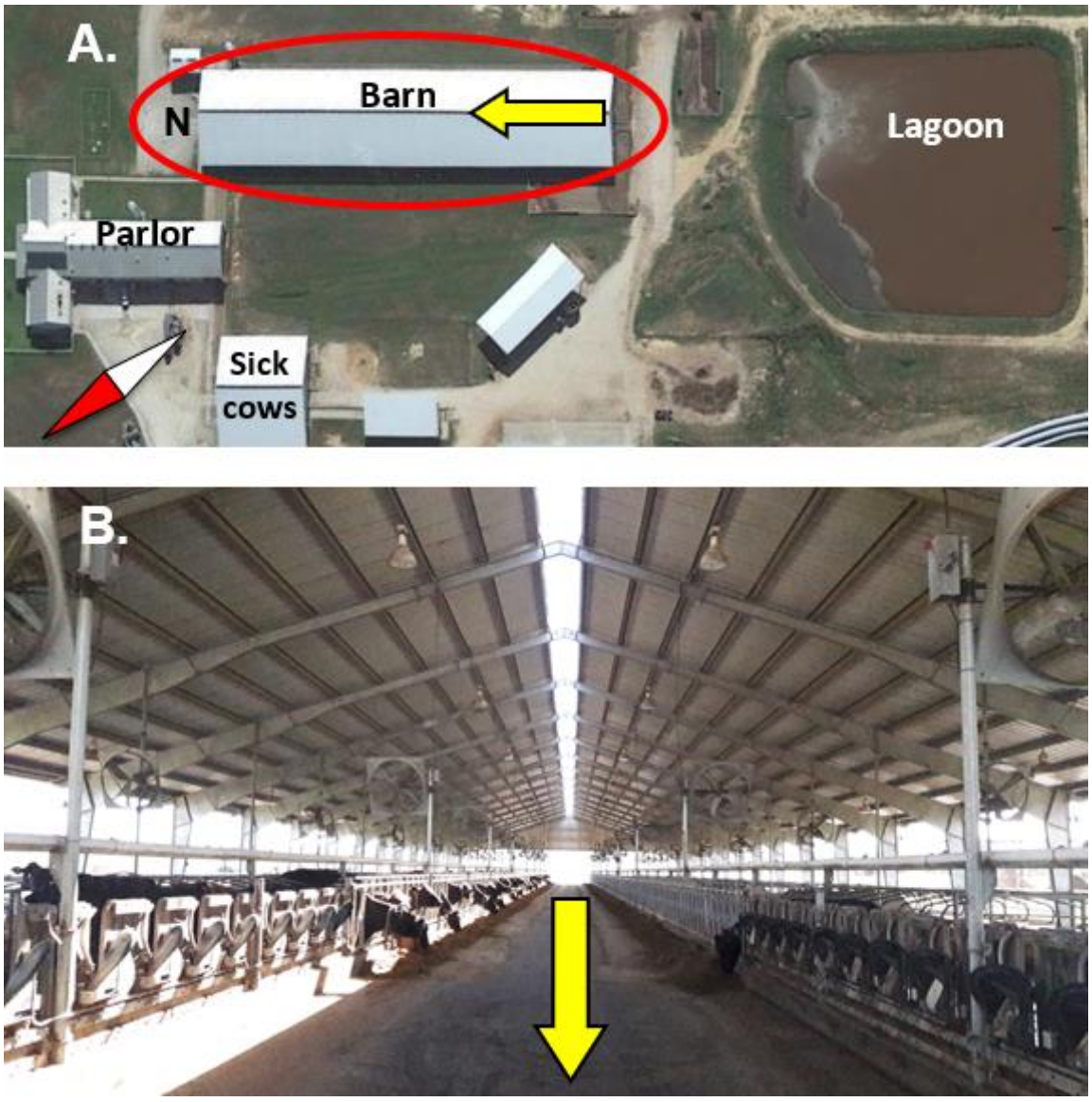

Figure 3.1 A. Open stall dairy facility. Red circle indicates the barn where samples were collected. B. Inside view of dairy barn. Arrow points towards north. N indicates north.

3.2. Sample collection

In all sampling campaigns, 15 aerosol samples and 10 manure samples were collected at the respective locations shown on Figure 3.2. Wetted Wall Cyclones (WWCs)

(Figure 3.3) was utilized for aerosol collection as it could continuously collect bioaerosols with an average collection efficiency over 86 % (McFarland et al., 2010). The WWC sampling collected aerosols at a rate of 100 L/min for 15 minutes into 50 mL Falcon tubes prefilled with a solution of milli-Q (MQ) water and 10 % phosphate buffer saline (PBS) to increase survivability of aerosolized bacteria. Dairy manure samples were manually collected into 50 mL Falcon tubes. Collected aerosol and manure samples were immediately stored in an ice box. A HOBO data logger (U12-013, Onset, Bourne, MA) was placed in each location for 15 minutes to record temperature and relative humidity (RH). Measurements were taken every five seconds throughout the collection period with an accuracy of ± 0.35 °C and ± 2.5 % RH, respectively. Weather data was obtained from a weather station (Crop Link Pro, Valley, Omaha, NE) that was located at the dairy facility. Air velocities were also measured in each location using a hot-wire anemometer (Model 8360, TSI Inc., Shoreview, MN, USA) at heights of 0.8 m and 1.5 m above the ground representing the heights of cows laying down and standing up, respectively. Measurements were taken every 6 seconds for a minute, three times, resulting in 30 air velocity measurements recorded in each location and height.

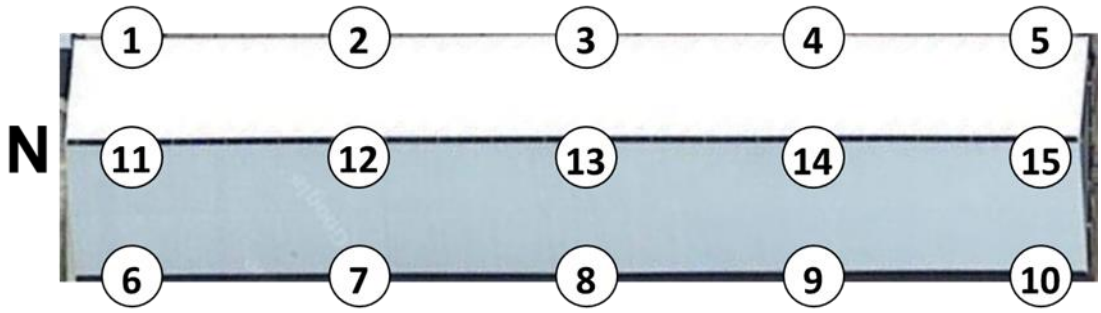

Figure 3.2 Locations where aerosol and manure samples were collected. N indicates north.

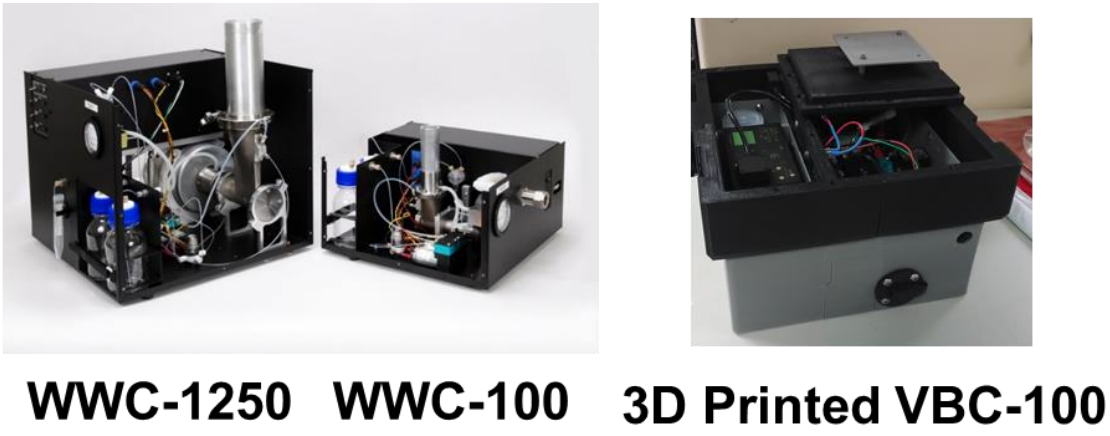

Figure 3.3 Wetted Wall Cyclone sampling systems used for aerosol sample collection.

3.3. Kirby-Bauer disk diffusion test

An aliquot of manure and aerosol samples were plated on tryptic soy agar (TSA, Becton Dickinson) plates on the day of sampling and incubated at 37 °C overnight. The colonies were then streak-plated on another set of plates and tested for antibiotic resistance using the Kirby-Bauer test. The eight antibiotic disks that were used in this test and their concentrations are listed in Table 3.1. The zone of inhibition was measured and compared

using the standards from Clinical and Laboratory Standards Institute to determine if the bacteria was susceptible, intermediately resistant, or resistant to different antibiotics (CLSI, 2014). Each antibiotic has different diameter ranges for zone of inhibition to determine whether the bacteria demonstrate resistance or not. If the bacteria grew in between the resistant (R) and susceptible (S) ranges, they were classified as intermediately resistant (I).

Table 3.1 Minimum inhibitory concentration of antibiotic disks used for Kirby-Bauer disk diffusion test and zone of inhibition ranges for resistance

Antibiotics	Concentration (µg/disk)	Zone of inhibition (mm)		
		Resistant (R)	Intermediately resistant (I)	Susceptible (S)
Ampicillin (AM)	10	≤ 13	14 - 16	17 ≤
Cefoperazone (CFP)	75	≤ 15	16 - 20	21 ≤
Cephalothin (CF)	30	≤ 14	15 - 17	18 ≤
Imipenem (IPM)	10	≤ 19	20 - 22	23 ≤
Gentamycin (GM)	10	≤ 12	13 - 14	15 ≤
Tetracycline (TE)	30	≤ 11	12 - 14	15 ≤
Sulfamethoxazole-trimethoprim (SXT)	SX (23.75), T (1.25)	≤ 10	11 – 15	16 ≤
Ciprofloxacin (CIP)	5	≤ 15	16 - 20	21 ≤

3.4. DNA extraction

Bacteria DNA from each manure and aerosol sample were extracted using the alkaline lysis method (Zhou et al., 1990). First, cells were lysed in TENS buffer (10x TE buffer, 0.1M NaOH, 20 % SDS). Then proteins were precipitated by 3N sodium acetate and removed after centrifugation. Poly Acryl Carrier (PC152, Molecular Research Center Inc., Cincinnati, OH) was added to the supernatant and the DNA was precipitated using isopropanol. The DNA was centrifuged, isopropanol was discarded, and the pellet was washed with ethanol. Then the pellet was hydrated in DNAse-free Milli-Q water.

3.5. 16S rRNA sequencing

Isolated bacterial DNA from seven aerosol samples, four manure samples, one lagoon air sample, and one lagoon water sample from the three sampling campaigns were sent to the Texas A&M Institute for Genome Sciences and Society (TIGSS) for 16s rRNA sequencing using the Swift library preparation kit. DNA samples were quantified via high sensitivity dsDNA Qubit Fluorometric assay and checked with the Agilent Genomic DNA tape on the Agilent TapeStation. DNA samples were normalized to equal concentrations and then sequencing libraries were generated using the Swift Biosciences 16S +ITS amplicon sequencing library preparation kit following the manufacturer's protocol. Resulting libraries were quantified via qPCR using the KAPA Library Quantification Kit for Illumina specific libraries (Roche). Sample concentrations were normalized and used to produce an equimolar 4 nM library pool. This library pool was denatured and diluted to

a final loading concentration of ~8 pM and run on an Illumina MiSeq 2x250 v2 sequencing kit.

3.6. Microbiome analysis

Once the sequences were received in a fastq format, they were imported into the QIIME2 environment version 2019.1 and denoised using Divisive Amplicon Denoising Algorithm 2 (DADA2) to eliminate sequencing errors and chimeras (Callahan et al., 2016). Generated amplicon sequence variants (ASVs) were trained using naive Bayesian classifier and compared with SILVA database to obtain taxonomy information of bacteria (Pruesse et al., 2007). A phylogenetic tree was created to observe the alpha and beta diversity measures between samples. Faith's phylogenetic diversity was used to examine the number of species in a sample, or richness, and the Shannon index was used to investigate the richness and diversity, or proportion of species abundance, in a sample.

3.7. Computational fluid dynamics modeling

3.7.1. Design 3D model of dairy facility

A 3D model of the dairy barn was built in SolidWorks using the blueprint and additional information provided by the facility (Figure 3.4). The length and width of the facility was 139.1 m and 30.7 m, respectively. Height was 3.7 m on the side and 9.8 m in the center of the barn. There was an opening through the middle of the roof. For simplification of the CFD simulation, fences, poles, floor layers, and troughs were excluded from the model. To understand how air flow is affected by areas where cows are

clustered together, 10 simplified cow models were placed in the southern side of the barn (Figure 3.5). The cow geometry was taken from another research paper that compared different cow models in CFD simulations (R. Mondaca and Y. Choi, 2016). The model was then imported into ANSYS Fluent 2020 R1 and simulations were performed using the Grace cluster in the high performance research computing (HPRC) system.

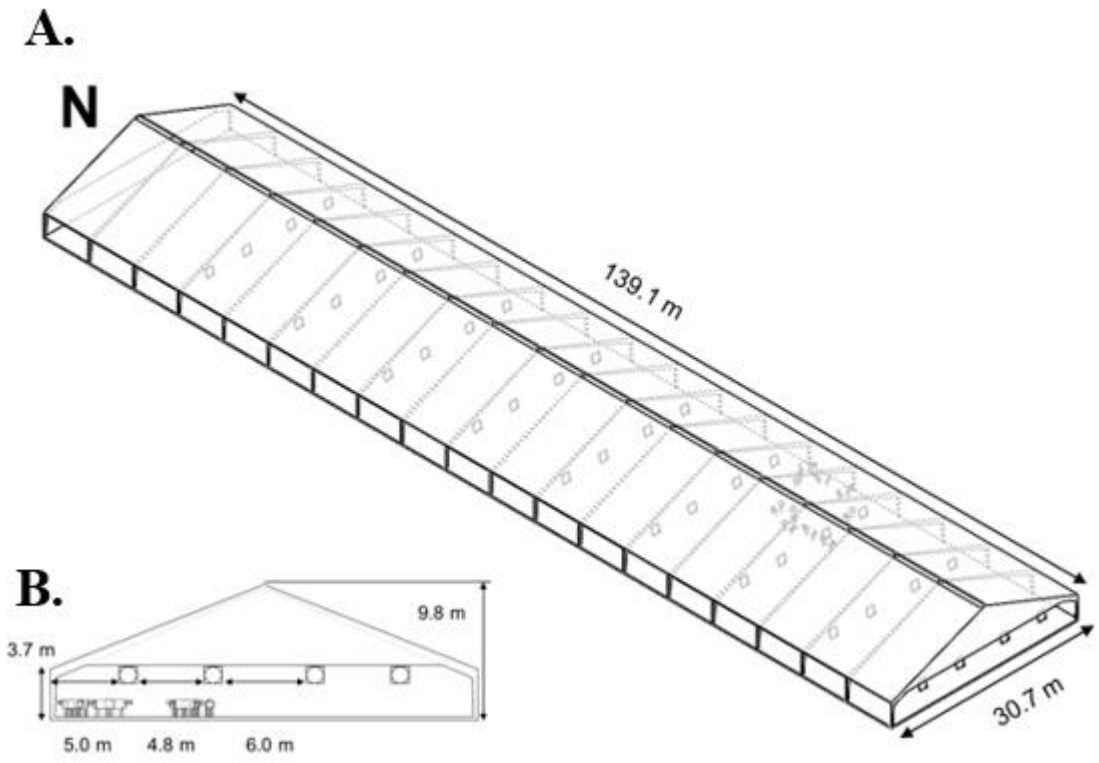

Figure 3.4 A. Isometric view of the dairy barn. B. Enlarged front view of the dairy barn seen from the north. N indicates north.

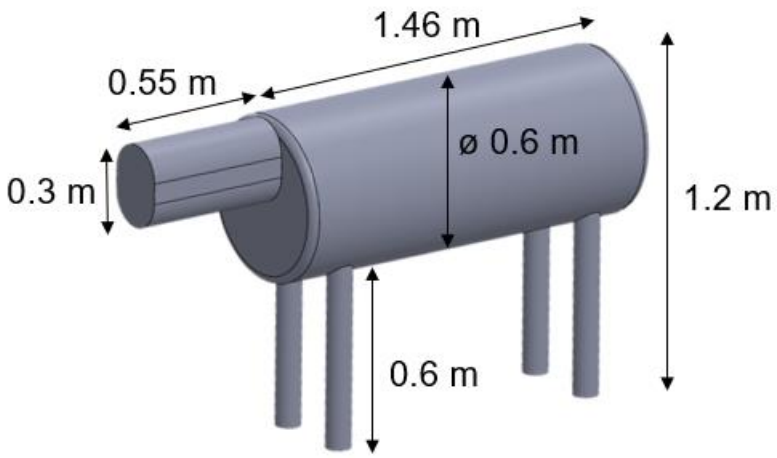

Figure 3.5 Dimensions of simplified cow model

3.7.2. Boundary domain

Weather data obtained in each sampling times indicated wind blowing from the environment at different speeds and directions. In order to incorporate this factor into the simulation, a boundary domain was built around the dairy barn. With the advancement of CFD techniques and wind tunnel experiments, different guidelines have been set up to design the computational domain (Franke and Baklanov, 2007; Tominaga et al., 2008). For a single building, it is recommended to set the inlet and top boundary at least 5H away from the building, where H represents the height of the building. For this CFD analysis, H was set to be 9.8 m. The outlet boundary should be at least 10H away from the building. For this research, wind flow directions were not parallel to the lateral boundaries, but at an angle. Therefore, two lateral boundaries were set as inlets at a distance of 6H, the other two lateral boundaries were set as outlets at a distance of 10H and the top boundary was set at 7H away from the building. Wind direction for Summer 2019 and Winter 2020 were

different from Spring 2021, so two different domains were used for the CFD simulation (Figure 3.6).

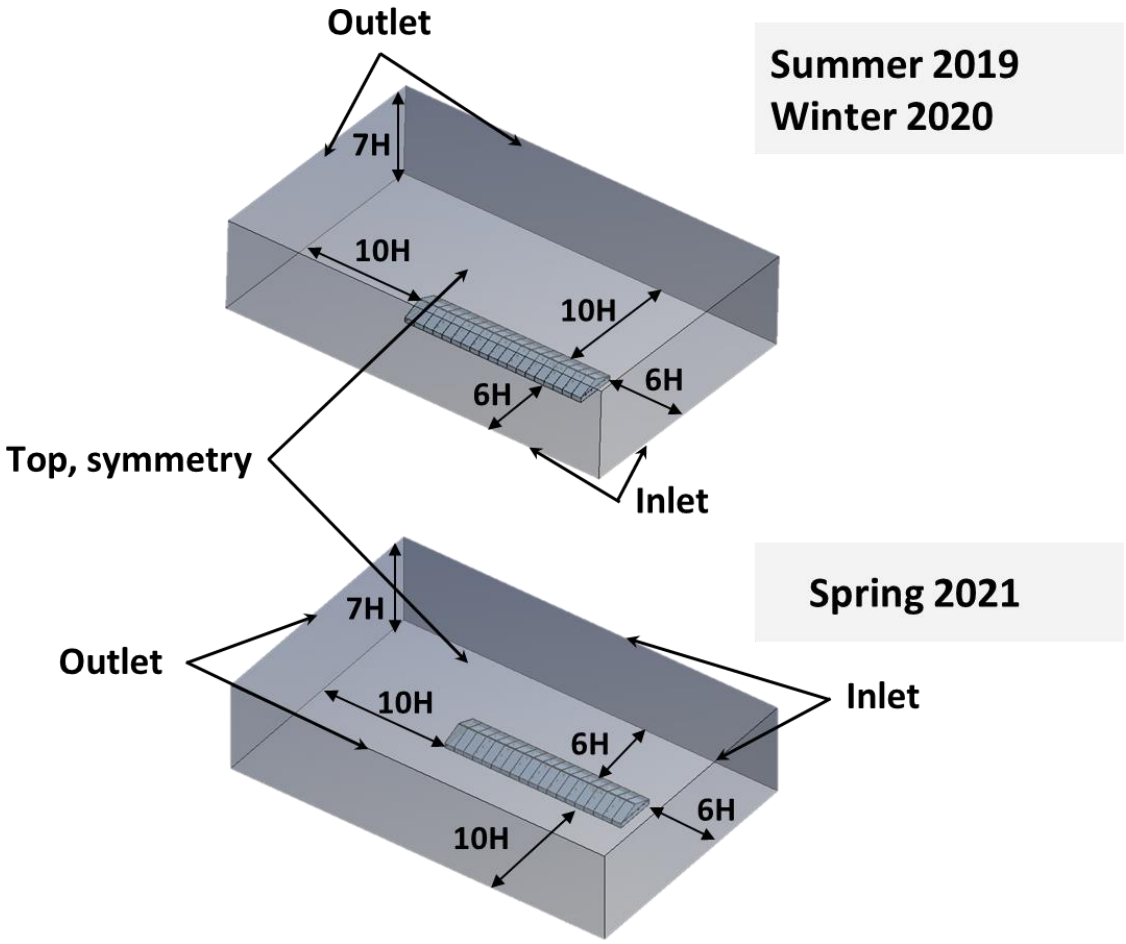

Figure 3.6 Two different computational domains for three sampling seasons. N indicates north.

3.7.3. Mesh

Three different meshes (coarse, medium, fine) were built for the three sampling times to analyze the grid convergence (Table 3.2). This is to ensure that the grid sizes are fine enough to not affect the results obtained from the CFD simulations. Cells were larger around the computational domain and became more refined along the dairy barn.

Tetrahedral cells were automatically generated in ANSYS using different grid sizes. Inflation layers were created on the floor and walls of the dairy barn. Face sizes around the fans and cows were refined to 0.05 m to more accurately simulate air flow properties (Figure 3.7). The tetrahedral cells were then converted into polyhedral cells to reduce the number of total cells by around 4-fold and ease the necessary computational processing power and time (Sosnowski et al., 2017).

Table 3.2 Grid sizes and total cell numbers for each simulation used to test grid converegence index

Sampling season	Grid size	Tetrahedral cells	Polyhedral cells
Summer 2019	Coarse	11,134,436	2,300,686
	Medium	16,932,162	4,841,176
	Fine	20,580,839	5,604,925
Winter 2020	Coarse	11,134,436	2,300,686
	Medium	16,936,051	4,841,753
	Fine	20,584,544	5,606,325
Spring 2021	Coarse	11,134,972	2,300,806
	Medium	16,954,347	4,857,777
	Fine	20,555,229	5,583,627

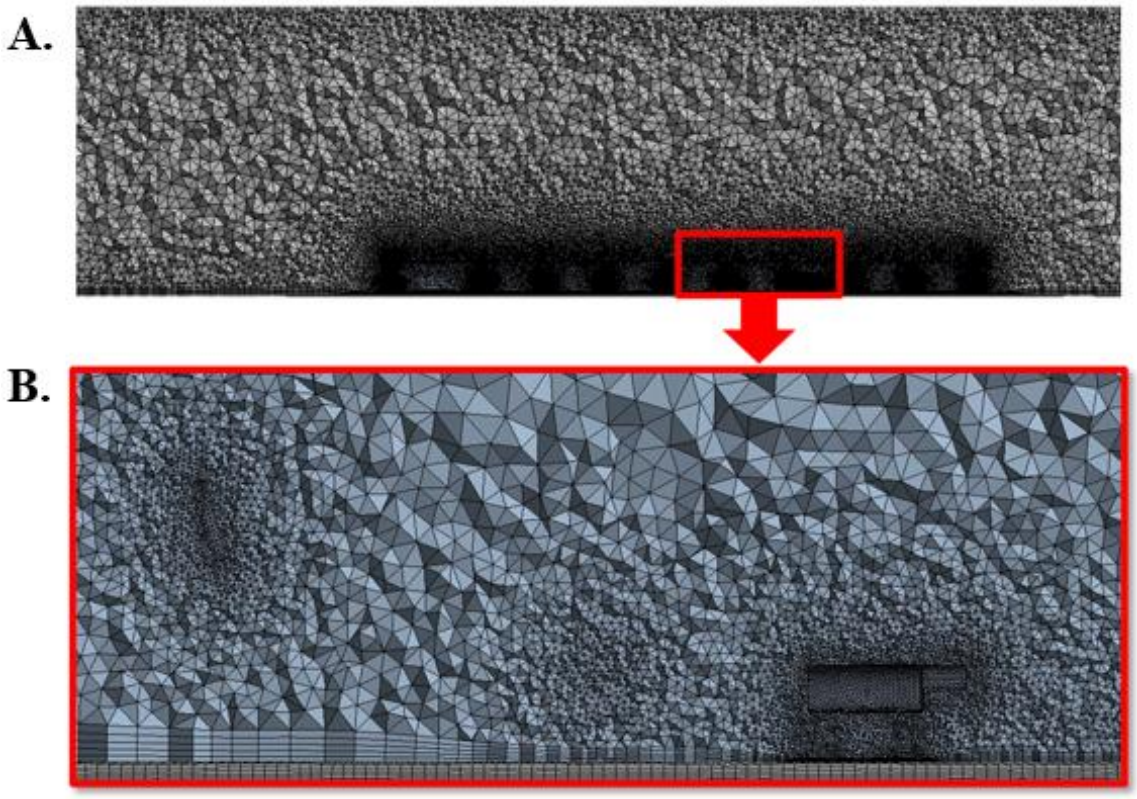

Figure 3.7 A. Mesh seen from the side. B. Close up mesh around the fans and cows.

3.7.4. Boundary conditions

The nine different models were imported to ANSYS Fluent to perform air flow simulations in steady state. The energy equation and realizable k-ε turbulence model with enhanced wall treatments were utilized. Wind velocities and directions for each season are stated in Table 3.3, along with the fan velocity if they were operational. Boundary conditions for the inlet velocity profile of the computational domain was calculated using the following power law:

$$U_y = U_{ref}\left(\frac{y}{y_{ref}}\right)^{\alpha} \quad (9)$$

where U_y is the velocity at height y, U_{ref} is the velocity at the reference height, y_{ref}, and α is the power law exponent. Here y_{ref} was set to 1.5 m and α was set to 0.14 according to another similar study (Tomasello et al., 2019).

Turbulent kinetic energy and dissipation rate profiles were calculated using Equations 2 and 3 to simulate a developed flow across the facility:

$$k = \frac{{U_*}^2}{\sqrt{C_\mu}} \tag{10}$$

$$\varepsilon = \frac{{U_*}^3}{K_v(y + z_o)} \tag{11}$$

where k is turbulent kinetic energy, ε is turbulent dissipation rate, U_* is friction velocity, K_v is von Karman's constant (0.4), C_μ is model constant, and z_0 is surface roughness length (Richards and Hoxey, 1993). Here C_μ was set to 0.09 and z_0 was set to 0.025 m (Ramponi and Blocken, 2012). Friction velocity was calculated using the following equation:

$$U_* = \frac{K_v U_{ref}}{\ln\left(\frac{y_{ref} + z_o}{y_{ref}}\right)} \tag{12}$$

Fan inlets were also set as velocity inlets. Outlets were set as pressure outlets and the top boundary was set as symmetry. Floors, walls, cows, and fans were set as walls with no-slip condition. The cow models were given a heat flux value of 205 W/m2 to mimic the heat generation from actual cow bodies. The SIMPLE solver was used along with a second order discretization scheme (Patankar and Spalding, 1972). Convergence was set to be achieved when the residuals for the continuity, velocities, kinetic energy, and turbulence energy dissipation were lower than 10^{-4} and the residuals for energy was lower than 10^{-6}.

Table 3.3 Velocities and direction of natural ventilation and fan velocity.

Time	Ambient velocity (m/s)	Wind direction	Fan velocity (m/s)
Summer 2019	4.25	WSW	8.3
Winter 2020	3.70	W	0
Spring 2021	0.36	SE	8.3

4. RESULTS

4.1. Microbiome diversity

The total relative abundance of phylum and genera richness in aerosol, manure, and lagoon samples for each of the three sampling seasons were combined and observed (Figure 4.1). Relative abundance of each individual sample collected at different locations and seasons are shown in Figure 4.2. The top 10 most common phyla and top 20 most common genera were identified from each sample. All other phyla and genera were grouped and labeled as "Other." These two plots of combined and individual relative abundance display an overview and detailed insight into the phylum and genera richness across different seasons and samples. In the phylum level, Firmicutes was most abundant (46 %), followed by Proteobacteria (31 %), Actinobacteriota (16 %), and Bacteroidota (4 %). The most abundant genera were *Bacillus* (37 %), *Acinetobacter* (21 %), *Sphingomonas* (7 %), and *Ruminococcaceae* UCG-005 (4 %).

A total of 5,561,995 sequence reads were denoised from 9,746,520 raw sequences imported from all the aerosol, manure, and lagoon samples. The highest read was 632,921 reads in aerosol sample from location 15 in Winter 2020 while the lowest was 10,459 reads in manure sample from location 6 in Spring 2021. Out of the aerosol samples, Winter 2020 had the highest read of 2,972,547, followed by Summer 2019 with 1,013,373 reads and Spring 2021 with 236,463 reads. The reads were clustered into 1,829 ASVs, 45 phyla, and 790 genera. The number of total genera in aerosol samples from Summer 2019, Winter 2020, and Spring 2021 were 431, 13, and 338, respectively. This shows that although

Winter 2020 aerosols had the highest denoised sequence reads, or richness, they did not have the most diverse taxonomic classifications. In manure samples from Summer 2019, Winter 2020, and Spring 2021, the total sequence reads were 685,582, 77,707, and 58,423 respectively, while the number of genera were 226, 169, and 137, respectively. A total of 132,714 reads and 152 genera were generated for lagoon aerosol samples while lagoon water samples had 128,188 reads and 353 genera.

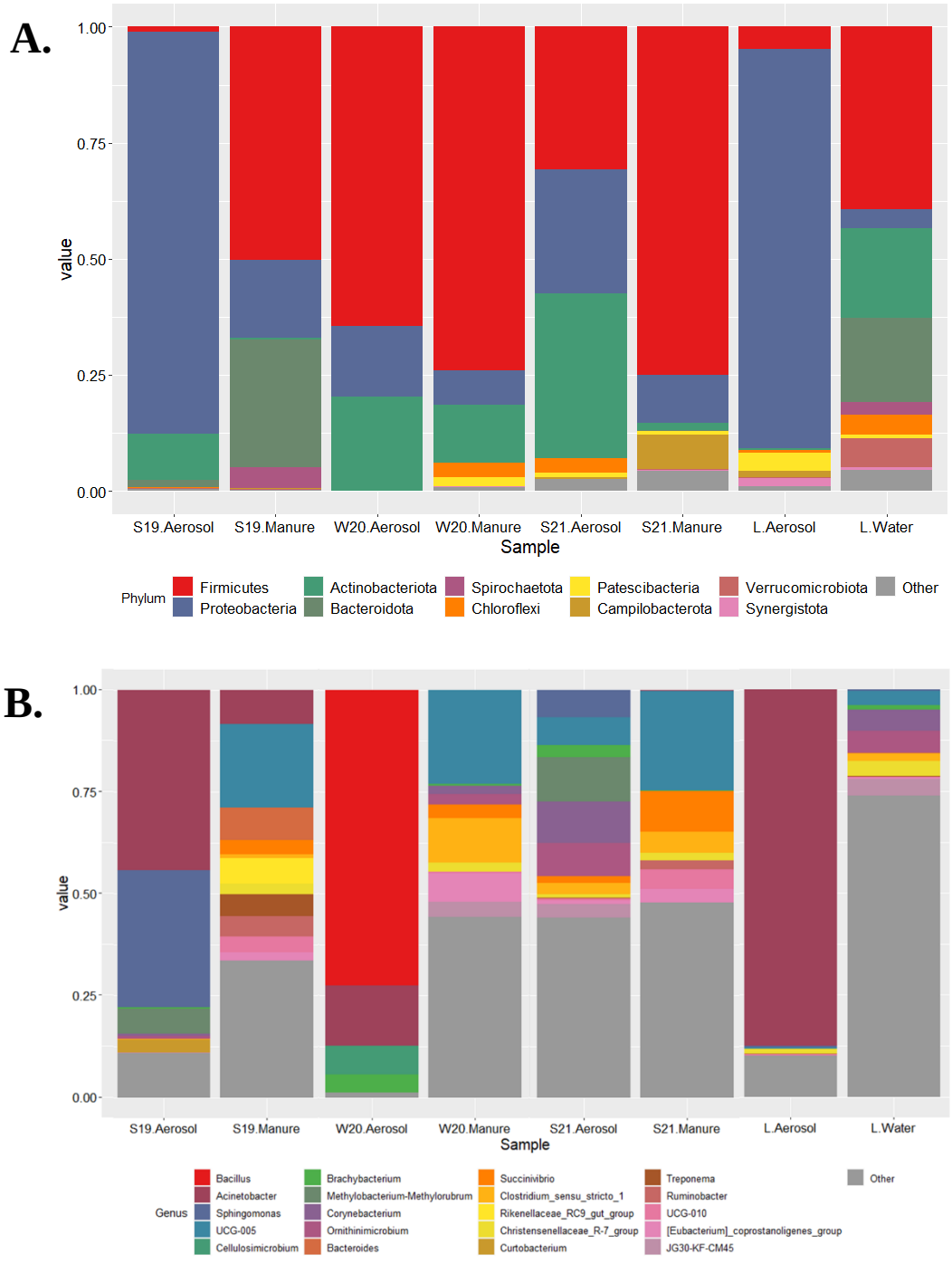

Figure 4.1 Total relative abundance of A. top 10 phyla and B. top 20 genera in aerosol, manure, and lagoon samples from different seasons. S19 - Summer 19, W20 - Winter 20, S21 - Spring 21, L – lagoon.

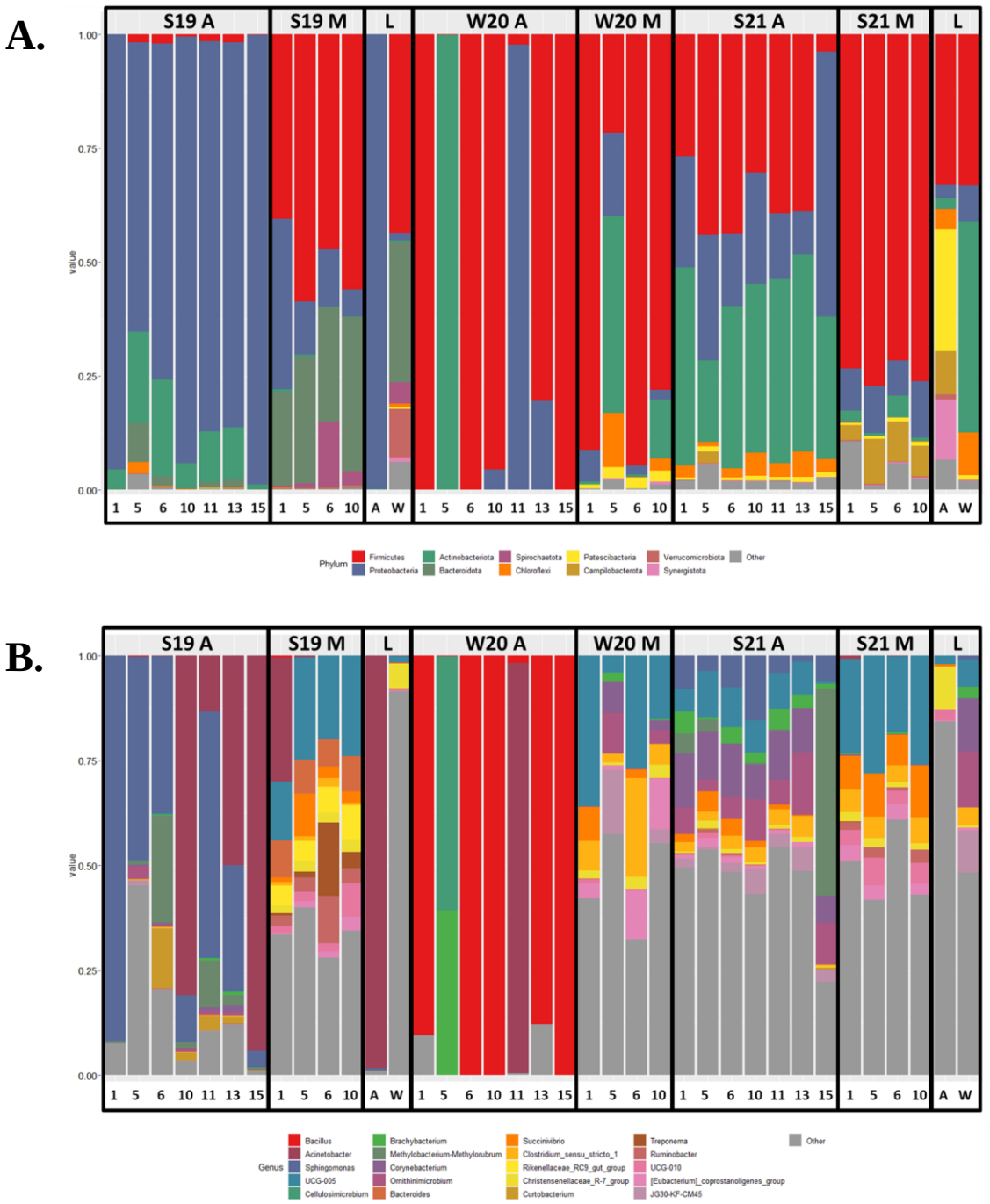

Figure 4.2 Relative abundance of A. top 10 phyla and B. top 20 genera in aerosol, manure, and lagoon samples from different seasons. S19 - Summer 19, W20 - Winter 20, S21 - Spring 21, L – lagoon, A - aerosol, M – manure. Numbers indicate locations in dairy barn where samples were collected.

An alpha rarefaction curve was produced to discern the required sequencing depth to estimate the total bacterial taxonomic diversity in the samples (Figure 4.3). Since the lowest sequence read was slightly above 10,000 reads, this was set as the sampling depth. It was shown that 10,000 sequences could sufficiently display most of the taxonomic diversity in the samples across seasons, indicated by plateauing of curves. As was depicted by the relative abundance, Winter 2020 aerosol samples had the lowest diversity while Summer 2019 manure samples had the highest diversity. Alpha diversity comparison using Shannon index revealed that there was a significant difference ($P < 0.05$) in the richness and diversity of aerosol and manure samples in all three seasons (Figure 4.4). The Bray-Curtis dissimilarity metric was used to create a principal coordinate analysis (PCoA) plot (Figure 4.5). It could be observed that aerosol and manure samples in Summer 2019 were clustered closely together as were the samples from Spring 2021. Aerosol and manure samples collected in Winter 2020, however, did not form a cluster, but showed a more dispersed pattern, signifying that they had dissimilar microbiome diversity.

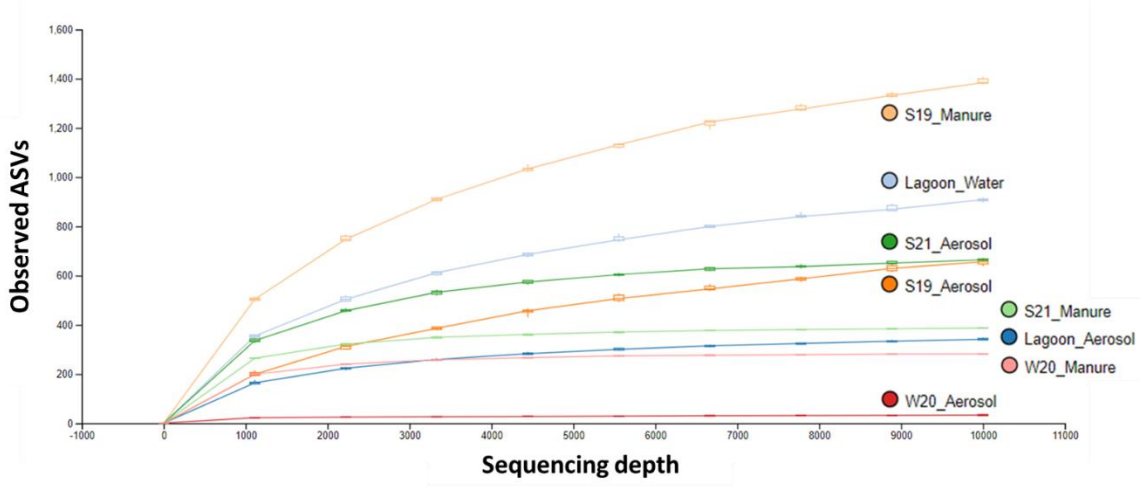

Figure 4.3 Alpha rarefaction curve of aerosol, manure, and lagoon samples from different seasons. This indicates that around 7,000 sequence reads were sufficient to display the majority of taxonomic profile in each sample.

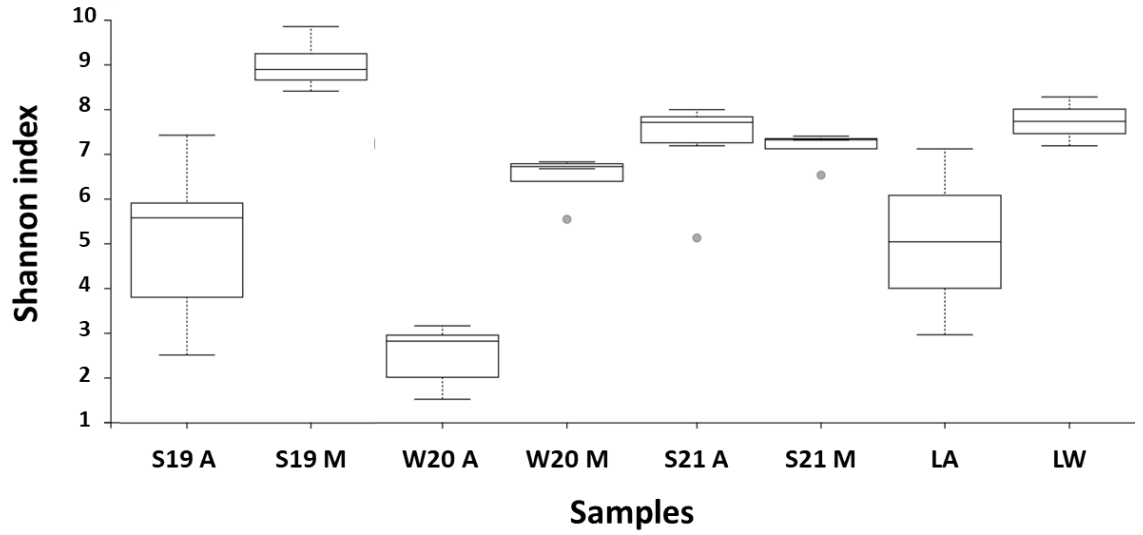

Figure 4.4 Alpha diversity measure comparison using Shannon index among aerosol, manure, and lagoon samples from different seasons.

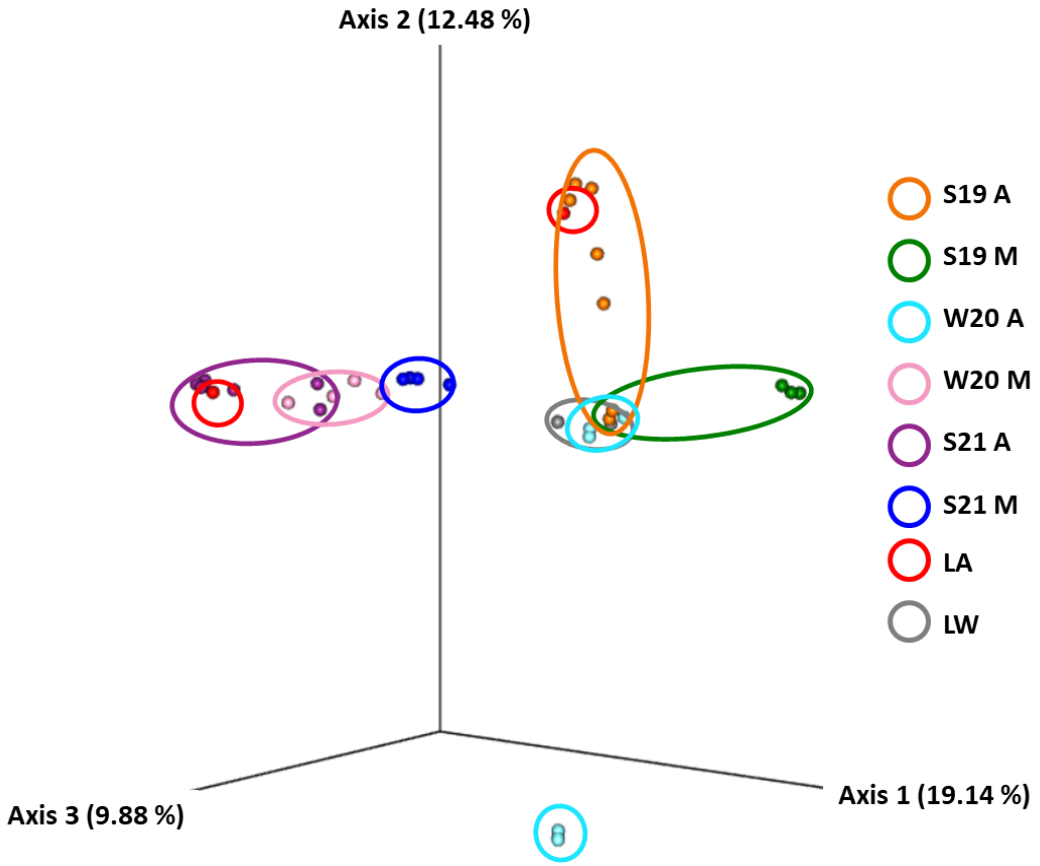

Figure 4.5 Beta diversity measure comparison using Bray-Curtis metric among aerosol, manure, and lagoon samples from different seasons.

4.2. Environmental measurements

Temperature and relative humidity measurements for all three visits were plotted and compared in Figure 4.6. The average temperature measurements for Summer 2019, Winter 2020, and Spring 2021 were 28.2 °C, 13.2 °C, and 26.4 °C, respectively, and relative humidity measurements were 59.5 %, 53.4 %, and 59.0 %, respectively. From the weather data obtained from the dairy facility, it was shown that the average temperature for the three seasons were 27 °C, 13 °C, and 22 °C, respectively, which closely matched with the HOBO data logger measurements. High fluctuations of temperature and relative

humidity measurements were observed in Summer 2019 at different locations. The sunlight during sample collection was directed mostly to the eastern and southern side of the barn. Therefore, temperature values were higher in locations 1 through 5, and 10, where there was most sunlight. This trend was also observed in Spring 2021 where locations 1 through 5 had the highest temperatures. Locations 11 through 15 were located in the center shielded from the sunlight by the ceiling and cows, resulting in a lower temperature.

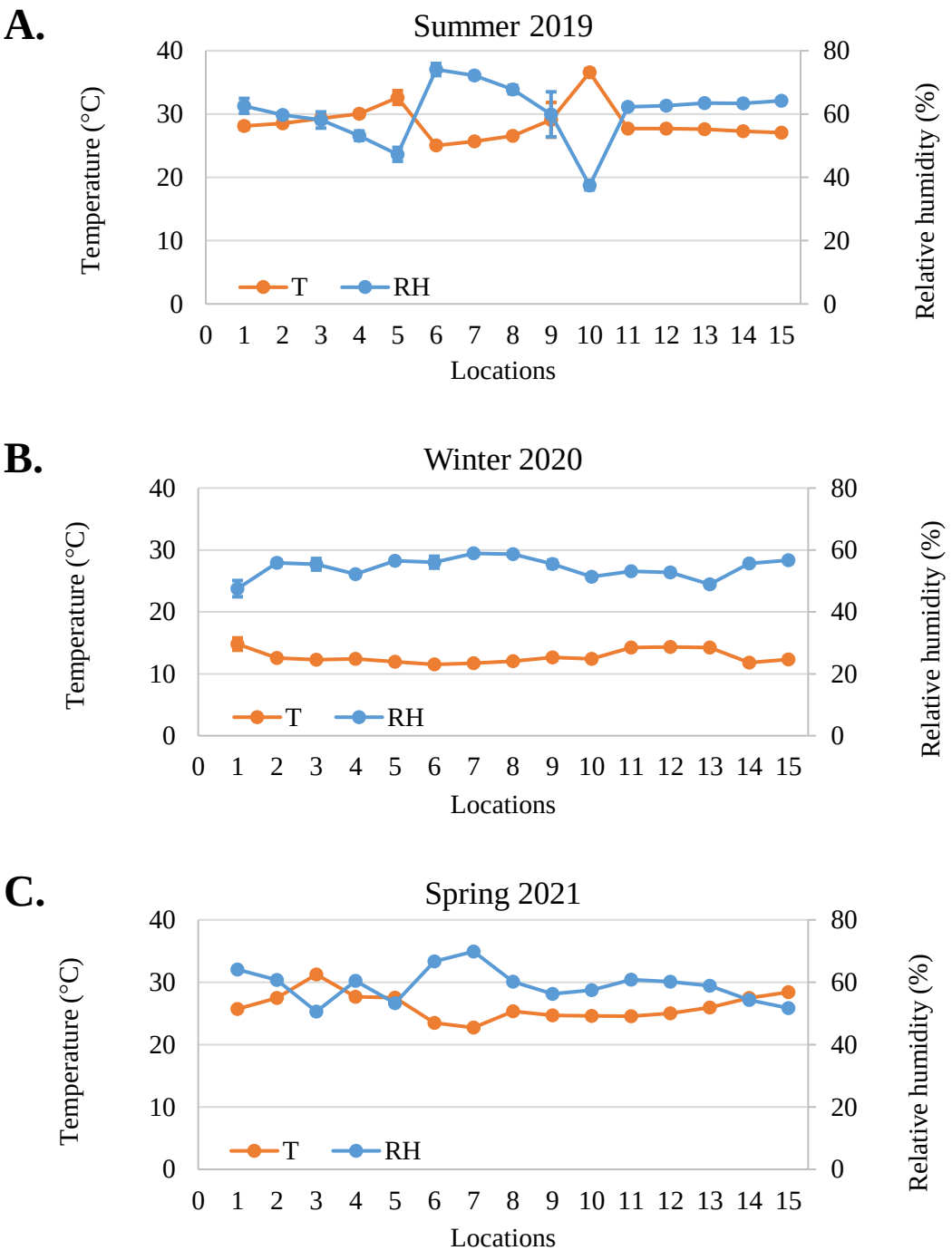

Figure 4.6 Temperature and relative humidity measurements recorded during bioaerosol sample collection at each location in A. Summer 2019, B. Winter 2020, and C. Spring 2021.

4.3. Antibiotic resistance test

A cumulative heatmap is shown in Figure 4.7. The resistance patterns of bacteria in bioaerosol and manure samples to different antibiotics for the three seasons are shown in Figures 4.8 and 4.9, respectively. Enlarged version of the radar charts can be seen in the Appendix. Throughout all three seasons, manure samples were consistently shown to be strongly resistant to all eight antibiotics. Aerosol samples, however, had different resistance patterns for each sampling period. For Summer 2019, aerosol samples collected from the southwestern side and center lane of the barn were more resistant than other aerosol samples. Strongest resistance pattern was shown diagonally from the southwestern to northeastern side of the barn, which aligned with the natural ventilation direction. Aerosol samples from Winter 2020 showed an overall similar pattern to that of Summer 2019, but the resistance against antibiotics were stronger in aerosol samples. Highest antibiotic resistance was shown in the southwestern side where wind from the environment was directly flowing into the barn. Spring 2021 aerosol samples had a unique antibiotic resistance mapping were almost all of the aerosol samples were specifically resistant against ampicillin and cephalothin. They also displayed less resistance towards majority of the antibiotics compared to Summer 2019 and Winter 2020 aerosol samples (Figure 4.8C). Antibiotic resistance in the manure samples were also slightly weaker than in the previous two seasons.

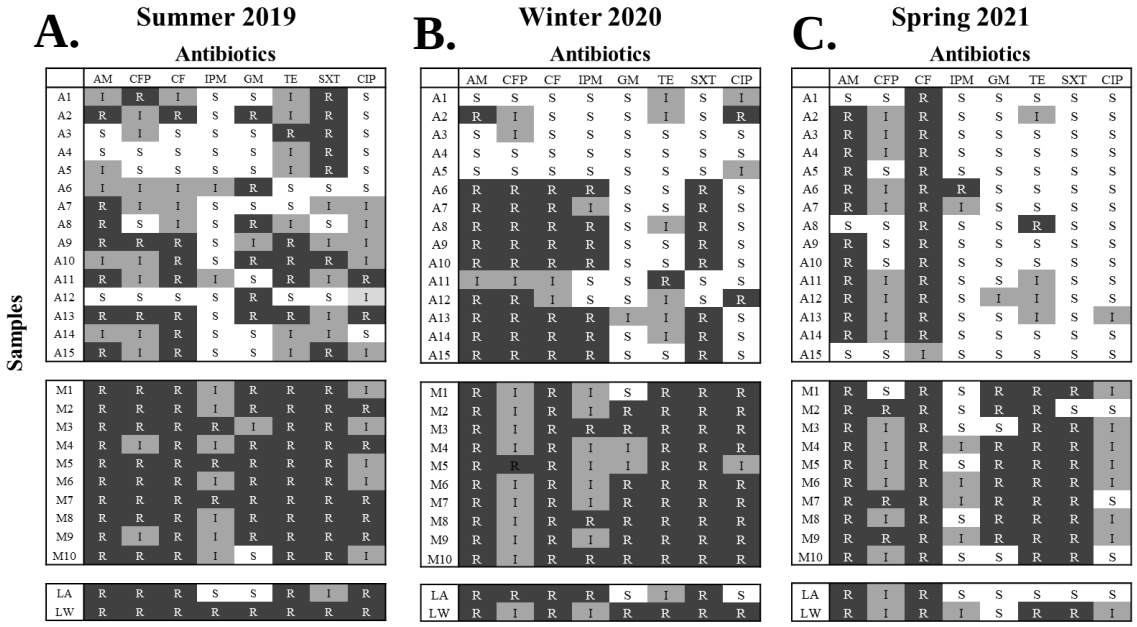

Figure 4.7 Antibiotic resistance heatmap in aerosol, manure and lagoon samples from different locations in A. Summer 2019, B. Winter 2020, and C. Spring 2021. A - aerosol, M – manure, LA – lagoon air, LW – lagoon water, AM – Ampicillin, CFP – Cefoperazone, CF – Cephalothin, IPM – Imipenem, GM – Gentamycin, TE – Tetracycline, SXT – Sulfamethoxazole-trimethoprim, CIP – Ciprofloxacin.

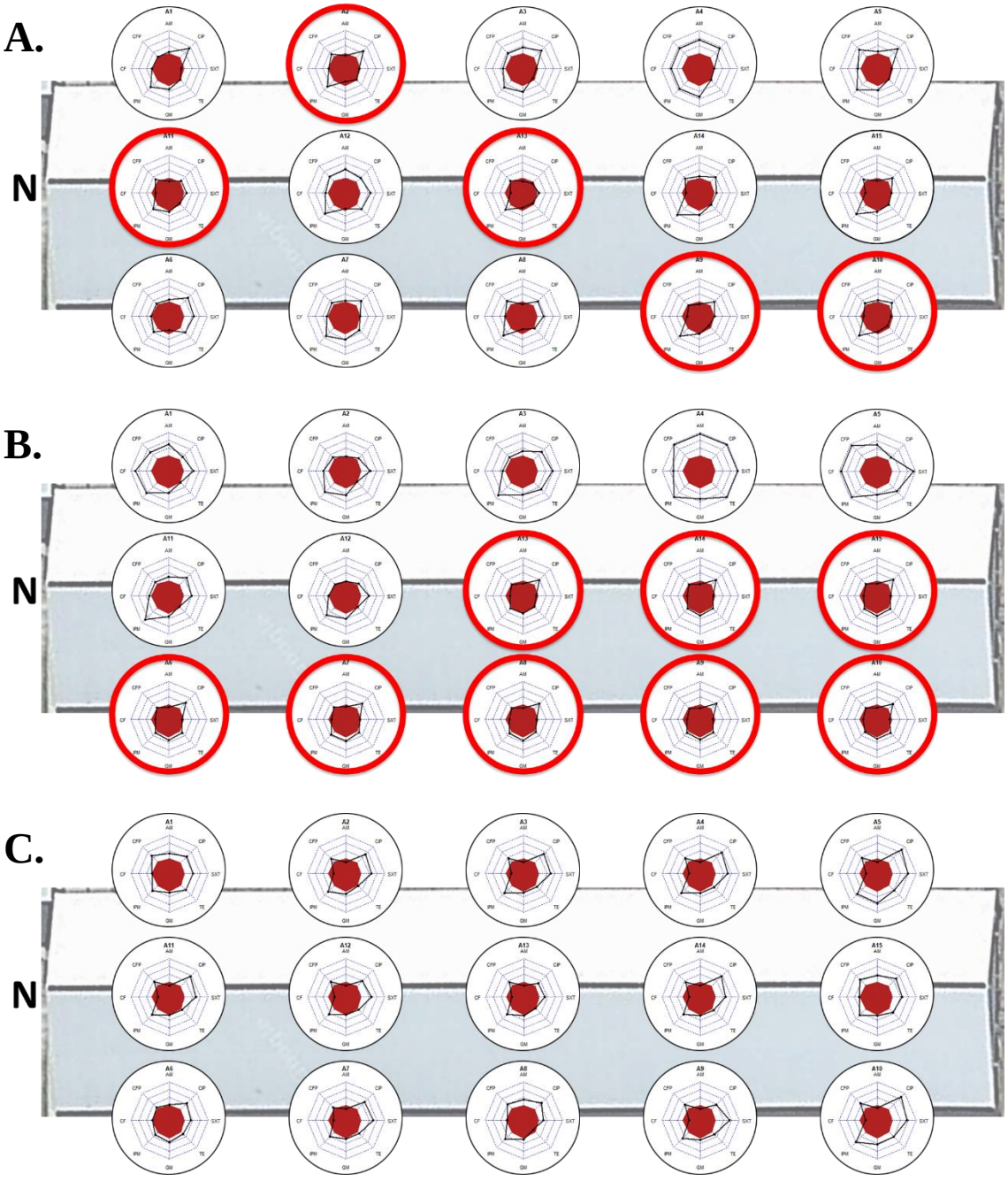

Figure 4.8 Antibiotic resistance pattern for aerosol samples in A. Summer 2019, B. Winter 2020, and C. Spring 2021. Samples that were resistant to four of more antibiotics are circled in red. N indicates north.

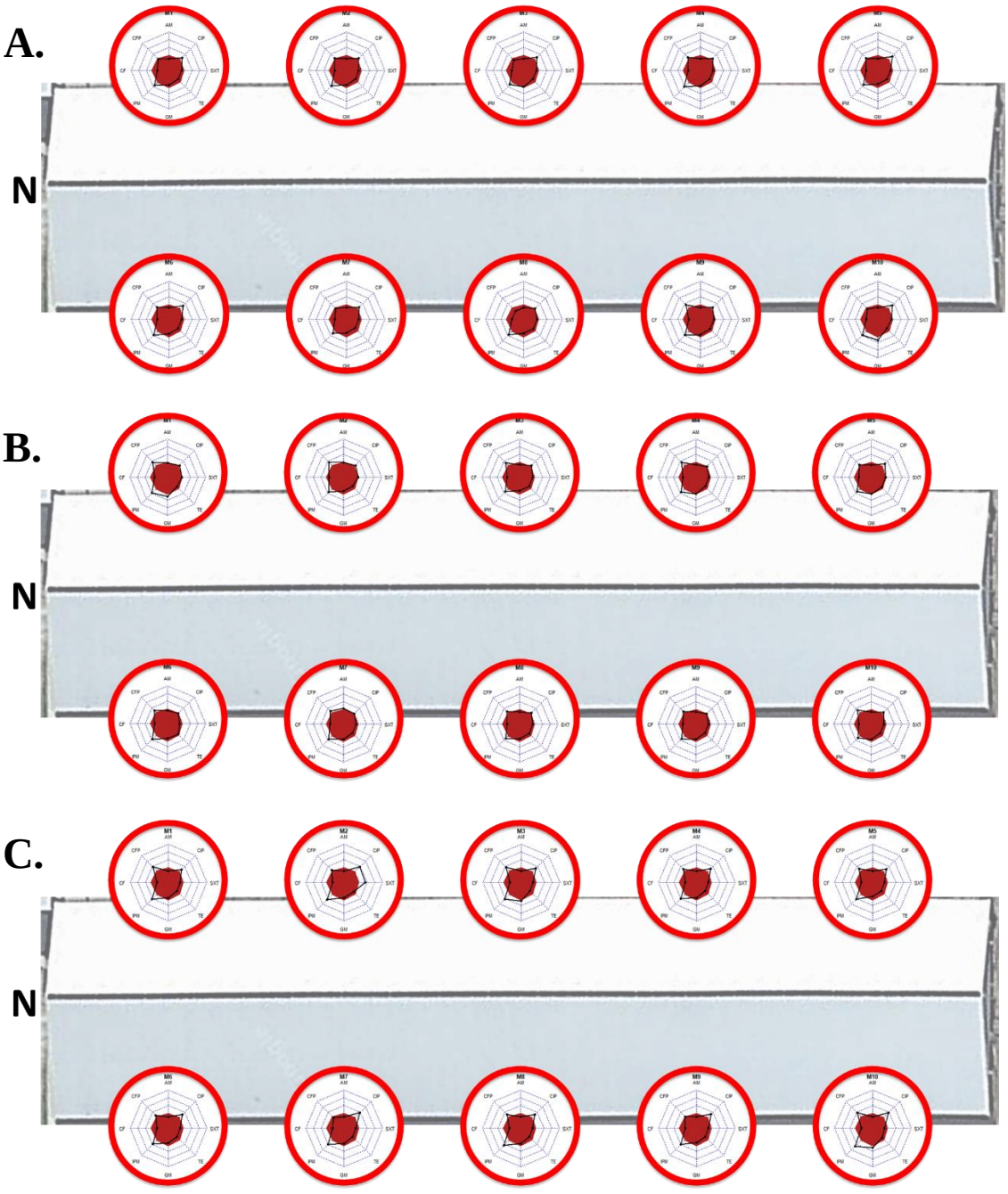

Figure 4.9 Antibiotic resistance pattern for manure samples in A. Summer 2019, B. Winter 2020, and C. Spring 2021. Samples that were resistant to four of more antibiotics are circled in red. N indicates north.

4.4. CFD simulation

4.4.1. Grid convergence index

The average number of iterations until the CFD simulations converged for Summer 2019, Winter 2020, and Spring 2021 were 845, 548, and 987 iterations, respectively. Average skewness and orthogonal quality were 0.781 and 0.218, respectively. Air velocity profiles from the floor to a height of 2.0 m in location 15 were compared in the three different grid sizes to examine grid convergence (Figure 4.10). It was shown that velocities for medium and fine mesh were well aligned, indicating that the different cell sizes resulted in the same output, while velocity profiles from the coarse mesh was slightly off from the other two. It was shown that the velocity profiles were developed consistent to the inlet boundary conditions. The medium mesh was shown to be sufficient enough for further analysis as it would require less computational processing power and cost, but reach the same results as the fine mesh simulations.

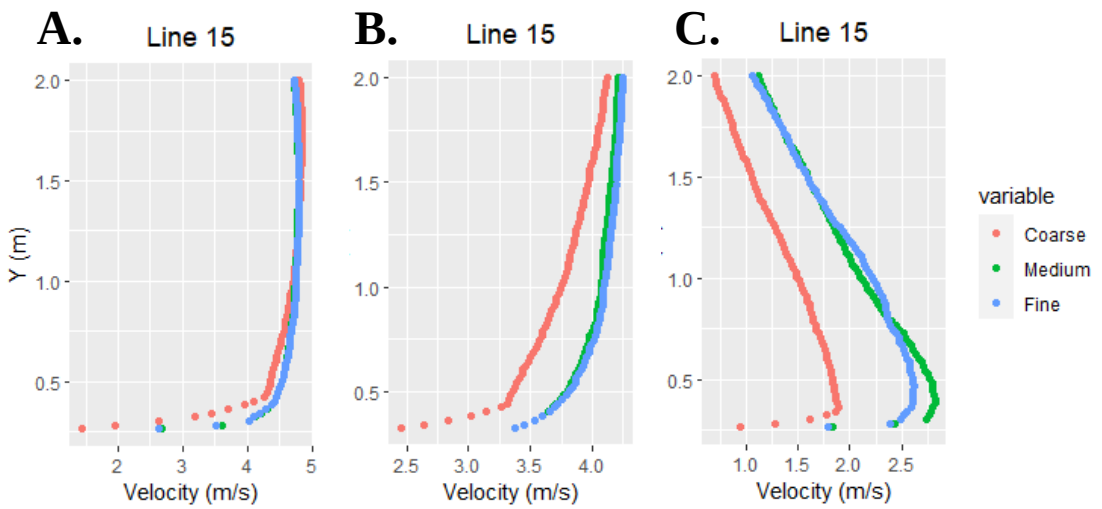

Figure 4.10 Grid convergence index of velocity profiles at location 15 from heights 0 to 2 m in A. Summer 2019, B. Winter 2020, and C. Spring 2021.

4.4.2. Air flow around dairy barn

Velocity contour maps were created to illustrate the air flow patterns over the computational domain and within the dairy barn. Figures 4.11, 4.12, and 4.13 show the velocity contours from the top of the barn at height of 1.2 m from the ground in Summer 2019, Winter 2020, and Spring 2021, respectively. Enlarged contour maps are also shown around the cow models to visualize how air flow behaves around them. Air velocity contours in Summer 2019 and Winter 2020 shared almost the same profile as the direction and magnitude of natural ventilation were similar to each other. However, as the fans were not operational in the winter, the top velocity contour for Summer 2019 and Winter 2020 are slightly different in direction and magnitude of air flow as it exits the dairy barn. Air flow in Spring 2021 were mostly generated by the 36 axial fans and slightly affected by the lower wind velocity from the environment. However, all three seasons' CFD

simulation indicated a turbulent region where the air velocities are drastically decreased as it moves around the cows.

Figure 4.14 shows the velocity contours from the west over the whole computational domain along the center of the barn for the three sampling seasons. Wind velocities were higher in Summer 2019 and Winter 2020 than in Spring 2021, which formed turbulent air movement as it contacted the dairy barn walls and ceiling in the southern and northern side. Similar turbulence was observed from the southern side of the barn (Figures 4.15, 4.16, and 4.17). As the developed natural ventilation reached the dairy barn, it was shown to form swirls and eddies along the walls and roof. This phenomenon was more turbulent in Summer 2019 and Winter 2020 as expected due to the faster wind velocity. High turbulence in the western side of the barn correlates with the antibiotic resistance mapping shown in Figure 4.8. It was demonstrated that CFD simulations with the right initial boundary conditions obtained from experimental results can accurately depict air flow simulations even in open environments.

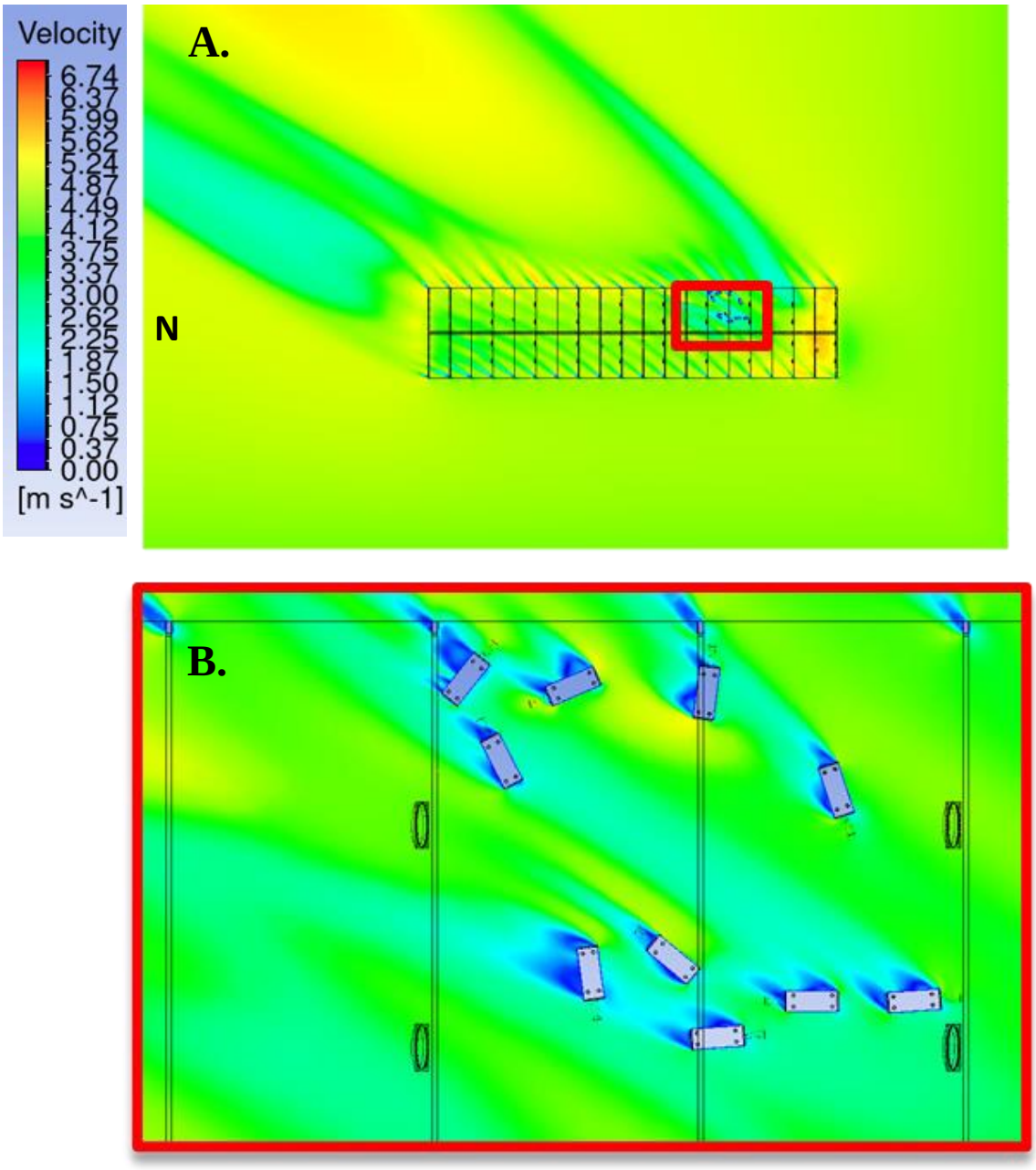

Figure 4.11 A. Velocity contour map over the whole computational domain shown from above at height of 1.2 m for Summer 2019. Red rectangle indicates where cow models were placed in CFD simulations. B. Enlarged velocity contour showing air flow dynamics around 10 simplified cow models. N indicates north.

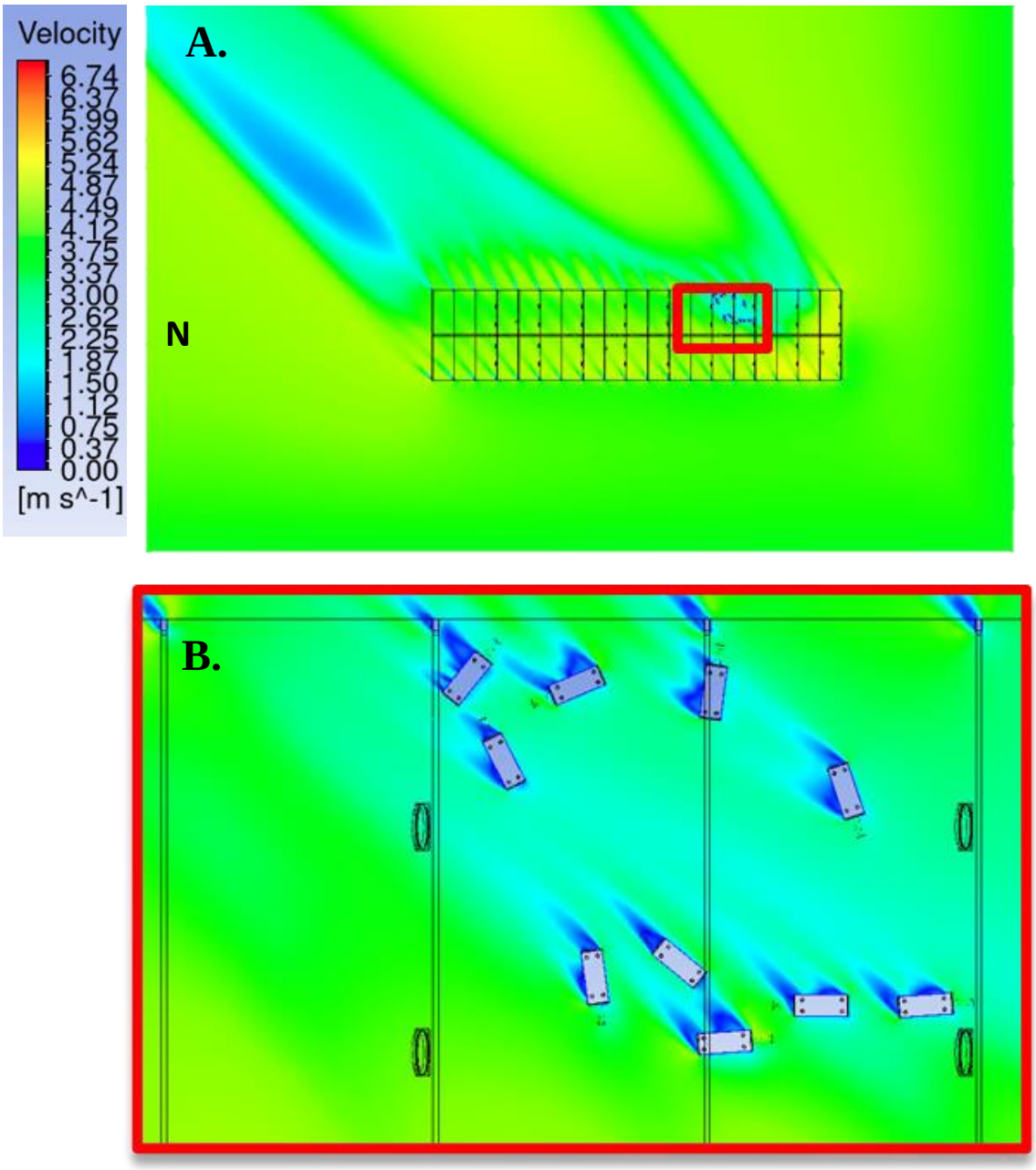

Figure 4.12 A. Velocity contour map over the whole computational domain shown from above at height of 1.2 m for Winter 2020. Red rectangle indicates where cow models were placed in CFD simulations. B. Enlarged velocity contour showing air flow dynamics around 10 simplified cow models.

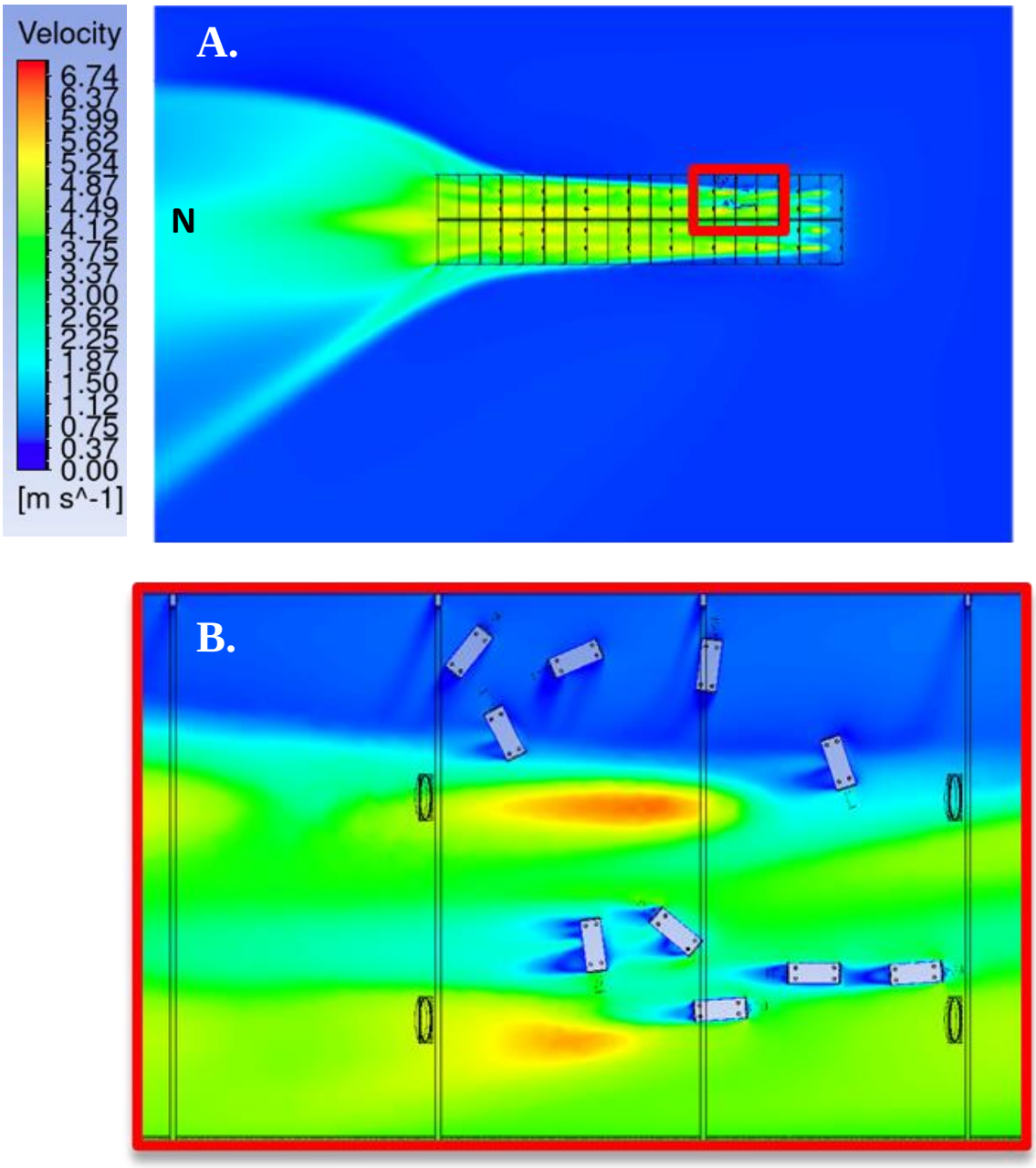

Figure 4.13 A. Velocity contour map over the whole computational domain shown from above at height of 1.2 m for Spring 2021. Red rectangle indicates where cow models were placed in CFD simulations. B. Enlarged velocity contour showing air flow dynamics around 10 simplified cow models.

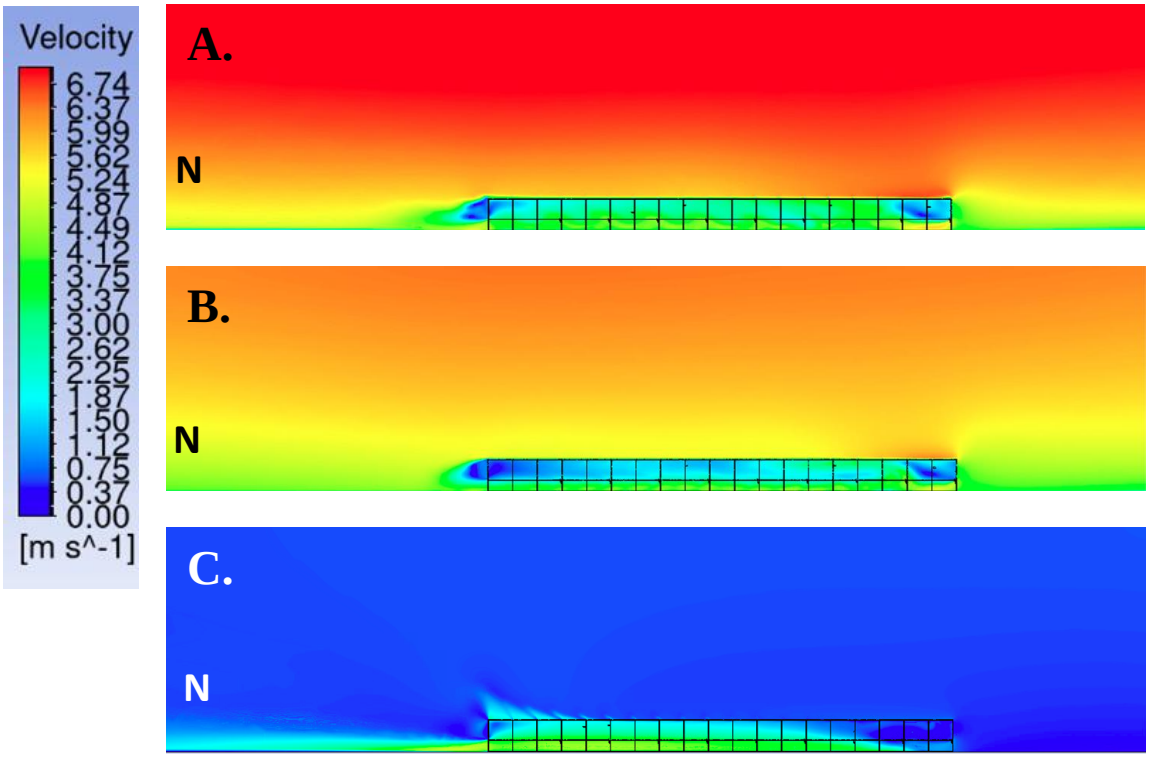

Figure 4.14 Velocity contour maps shown over the whole computational domain from the west along the center of the dairy barn in A. Summer 2019, B. Winter 2020, and C. Spring 2021.

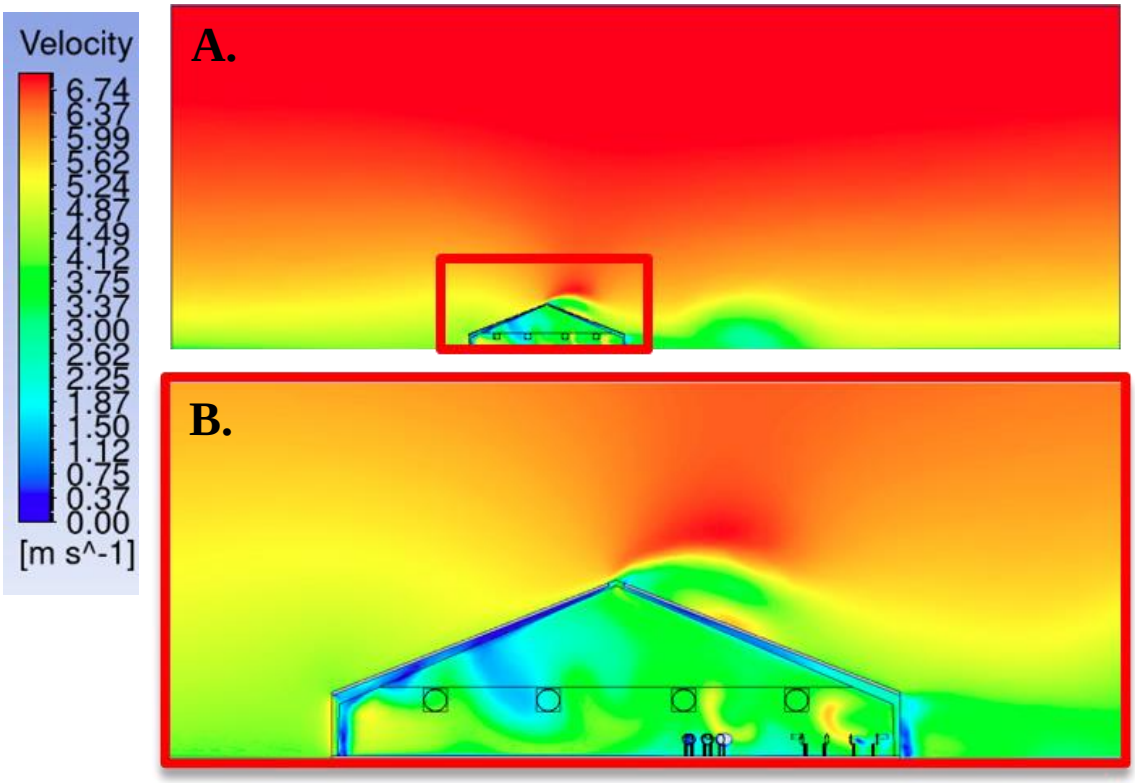

Figure 4.15 A. Velocity contour map over the whole computational domain shown from the south where the cows were located in Summer 2019. B. Enlarged velocity contour showing air flow dynamics around the barn walls, ceilings, and cow models.

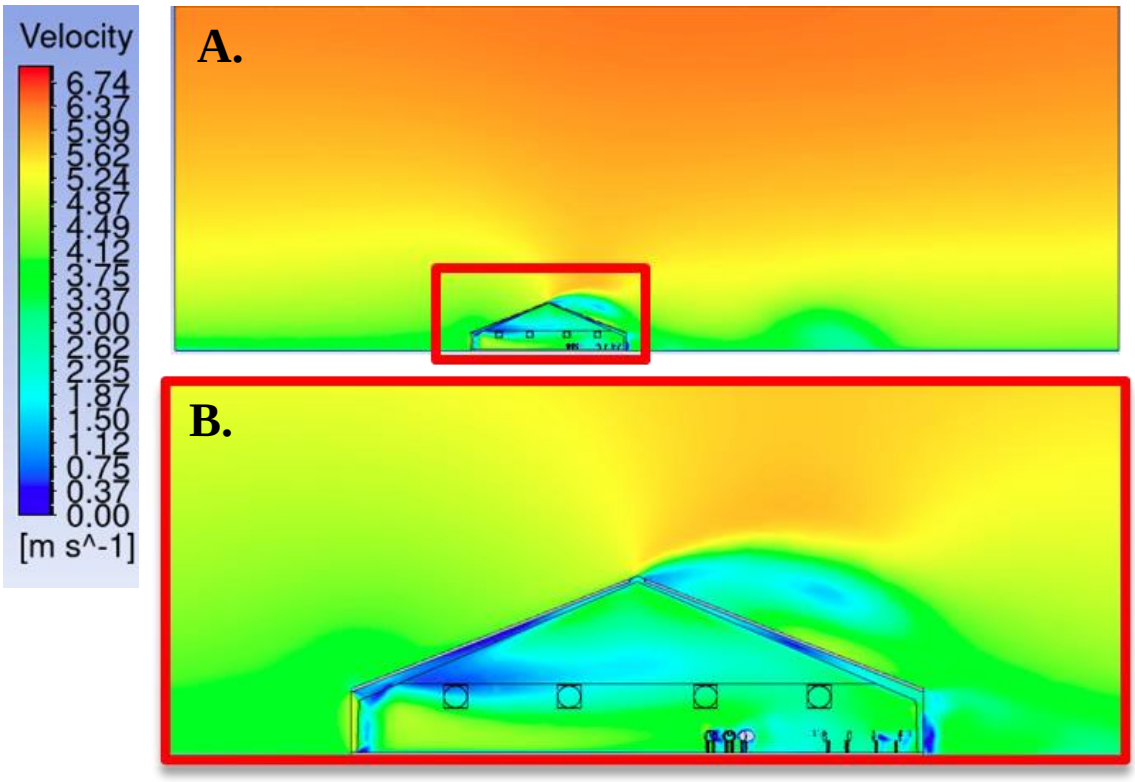

Figure 4.16 A. Velocity contour map over the whole computational domain shown from the south where the cows were located in Winter 2020. B. Enlarged velocity contour showing air flow dynamics around the barn walls, ceilings, and cow models.

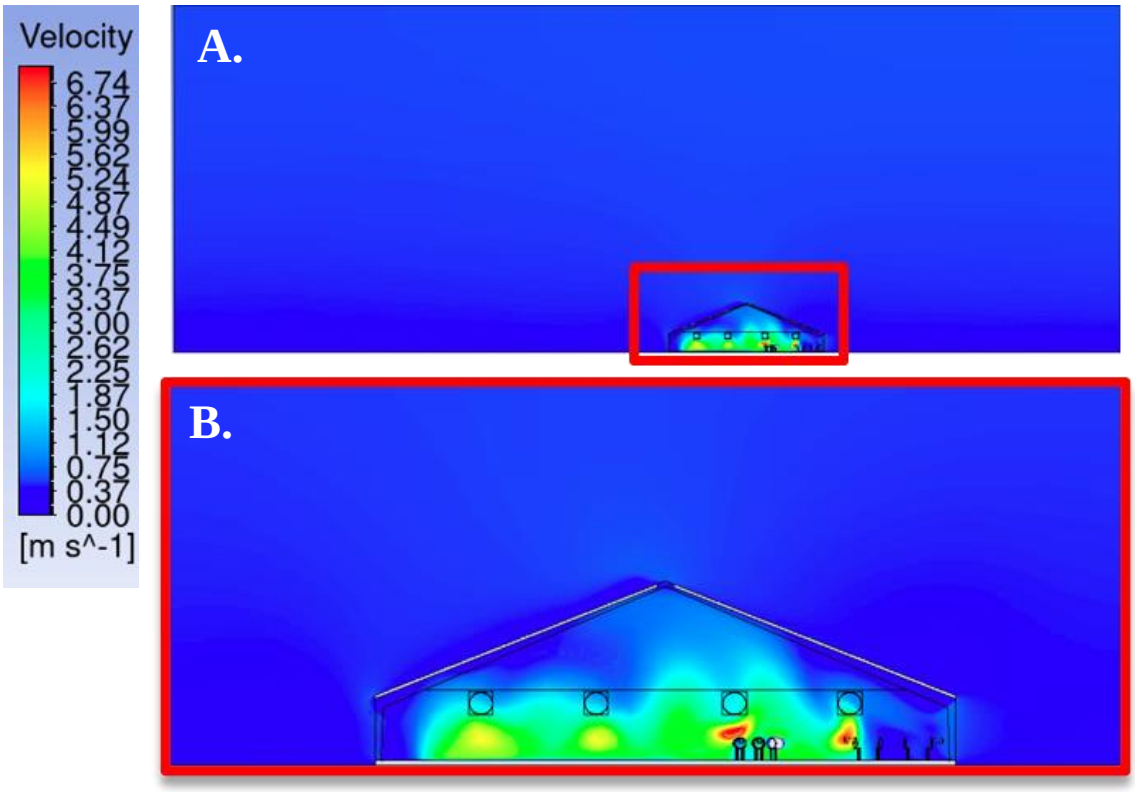

Figure 4.17 A. Velocity contour map over the whole computational domain shown from the south where the cows were located in Spring 2021. B. Enlarged velocity contour showing air flow dynamics around the barn walls, ceilings, and cow models.

5. DISCUSSION

5.1. Effect of seasonal and environmental factors on microbiome diversity

Microbiome diversity of aerosol, manure, and lagoon samples were investigated separately and in relation to the seasonal and environmental factors. It was observed that the manure samples in Summer 2019, Winter 2020, and Spring 2021 had similar microbiome diversity in the genera level. This was not the case for aerosol samples as their microbiome composition and diversity were significantly different from each other ($P < 0.05$). Also, only Spring 2021 aerosol and manure samples showed similar diversity, while Summer 2019 and Winter 2020 samples displayed high dissimilarity ($P < 0.05$).

Sequenced bacterial DNA are assigned into taxonomy units called amplicon sequence variants (ASVs) that are very specific and can be used to classify their taxonomy according to their sequences. It is recommended that samples have at least 5,000 sequences to capture the alpha diversity within the microbiome (Lundin et al., 2012). For aerosol and manure samples collected in the dairy barn across three seasons, the minimum sequence depth was higher than 10,000, providing sufficient microbiome diversity within the samples. Winter aerosol and manure samples had the lowest diversity while Summer 2019 manure sample had the highest diversity. This indicates that the lower temperature, slightly lower relative humidity, and stronger wind were not favorable for a wide variety of aerosolized bacteria to survive in the environment.

Seasonal effects on the microbiome diversity have been studied in other dairy-related researches. It was shown that Firmicutes and Bacteroidota were the two

dominating phyla in bacterial communities found in dairy cows' rumen over the course of five consecutive seasons (Noel et al., 2017). They also were two of the four most prominent phyla in aerosol and manure samples in this research over three seasons. Another study indicated that rumen samples in summer had the highest diversity while winter season had the lowest diversity, which is in agreement with this research (Islam et al., 2021). This pattern of microbiome composition changes according to different seasons were also observed in dairy milk and feces samples (Li et al., 2020a; Nikoloudaki et al., 2021).

It was previously shown that lower temperature and higher relative humidity may form a protective measure for aerosolized bacteria and increase their survivability when they become aerosolized (Marthi et al., 1990). Another study showed that increasing temperature decreased the relative recovery rates of E. coli and B. subtilis as they become inactivated with the rising heat (Jung et al., 2009). Although several studies demonstrated that temperature above 24 °C decrease the survivability of aerosolized bacteria, the exact effect of relative humidity is more unclear as it differs by their type (gram-negative, gram-positive, or intracellular) and method of culturing (Fernstrom and Goldblatt, 2013; Tang, 2009). Temperature in Winter 2020 was about 13 to 15 °C lower than Summer 2019 and Spring 2021, respectively, while relative humidity was lower by around 6 %. Results from KB test indicated that aerosols from Winter 2020 samples showed the most resistance against antibiotics compared to the other seasons, even though the overall microbiome diversity was lower. This could be due to the colder temperatures inducing mechanisms of survival in aerosolized bacteria that corresponds with antibiotic resistant mechanisms.

Another information worth noting is relative humidity and water content in aerosols. Relative humidity is often used to describe the amount of water vapor present in the air. The equation for calculating relative humidity is the amount of vapor pressure over the total saturation vapor pressure possible in a given temperature (Perry et al., 1997). Therefore, relative humidity is very dependent of temperature. A different parameter to look at water content in the air is vapor pressure. It was calculated that vapor pressure in Summer 2019, Winter 2020, and Spring 2021 corresponded to 2.28 kPa, 0.81 kPa, and 2.03 kPa, respectively, using measured temperature and relative humidity data. The amount of water content in the air or aerosol should be investigated more deeply as they control mass and heat transfer in aerosols (Cummings et al., 2020; Tan et al., 2017).

When cows were being milked, lagoon water was used to flood the floors to clean dairy manure. Water would flow from the northern side of the barn to the south as the floor was slanted in that direction. Because sunlight was shining directly towards the southern side, this accelerated the evaporation and aerosolization of accumulated flood water. There have been several studies on how direct sunlight causes inactivation of bacteria by damaging their cells and components (Ahmed et al., 2014; Hobday and Dancer, 2013; Nguyen et al., 2020; Tong and Lighthart, 1997). The intense and long exposure to sunlight on the southern side explains how additional environmental stress by sunlight could enable mechanisms of resistance against antibiotics were developed in aerosolized bacteria.

5.2. Antibiotic resistance mapping

It was observed that aerosol samples from Summer 2019 and Spring 2021 were susceptible to imipenem. Imipenem is a family of thienamycin that is sometimes administered with cilastatin. Its mechanism of action is to inhibit cell wall synthesis by binding to penicillin binding proteins and inactivating them (Rodloff et al., 2006). Ampicillin, cephalothin, and cefoperazone also inhibit bacterial cell wall synthesis and showed effectiveness in some aerosol samples, but they were not as effective in manure samples. Aerosol and manure samples from Winter 2020, however, showed strong resistance against imipenem.

Several of the identified bacteria genera were well known to be resistant to certain antibiotics. Bacteroidota, found in manure samples, produce beta-lactamases that provide resistant to antibiotics with beta-lactam rings, such as ampicillin and imipenem, although all manure samples from Summer 2019 were susceptible to imipenem (Wichmann et al., 2014). It could be that the type of beta-lactamase produced by the collected Bacteroides species were not resistant to imipenem. A different study revealed that Acinetobacter was resistant to cephalosporin, which is another beta-lactam antibiotic (Wepking et al., 2017). Although cephalosporin was not used in this study, the mechanism of resistant towards this antibiotic could have also caused resistance against other antibiotics. (Burgos et al., 2005) showed that Shigella found in dairy soil showed high resistance against chloramphenicol. Many of known ARB were detected in aerosol and manure samples at various locations and shown to be spreading to different locations throughout the dairy farm.

5.3. Comparison between experimental and simulation air velocity measurements

Air velocities at the 15 sampling locations in Summer 2019, Winter 2020, and Spring 2021 were compared with that from the CFD simulations. Although the dairy barn model was simplified to remove some obstacles, experimental and simulation data seemed to match in certain locations (Figure 5.1). For all three sampling seasons, air velocities closely matched in both outskirts of the barn (Locations 1 – 10), but the simulation air velocities were slightly higher in the center (Locations 11 – 15). This could be due to the obstacles, such as cows and troughs, blocking the air flow in real life to decrease the experimental air velocities in the center. For simplification and to reduce computational loads, these obstacles were removed and hence, simulation air velocities were slightly higher than experimental measurements inside the barn. However, air velocity measurements from CFD simulations around the barn fell closely within the ranges of experimental measurements as natural ventilation mainly affected these areas.

As shown in the weather data and CFD simulations, one major difference between Spring 2021 and the other two seasons was the velocity of natural ventilation. Average air velocity from the wind was 0.36 m/s in Spring 2021, while it was 4.25 m/s and 3.70 m/s for Summer 2019 and Winter 2020, respectively. The wind direction in spring was from the southeast while it was blowing from the west-southwest in summer and southwest in winter. Although all 36 fans were operational in Spring 2021, the weak ambient air velocity was not able to disseminate aerosolized bacteria far away from the dairy facility. However, Spring 2021 also had the most similar microbiome composition between the

aerosol and manure samples compared to other seasons as shown in Figure 4.2B. This could be an indication that lower air flow throughout the dairy facility enabled more collection of aerosols generated from the manure and flood water. Higher air velocities across the facility in Summer 2019 and Winter 2020 were shown to transport aerosolized and evaporated bacteria further away from the barn, leading more discrepancies to show up between the aerosol and manure taxonomy.

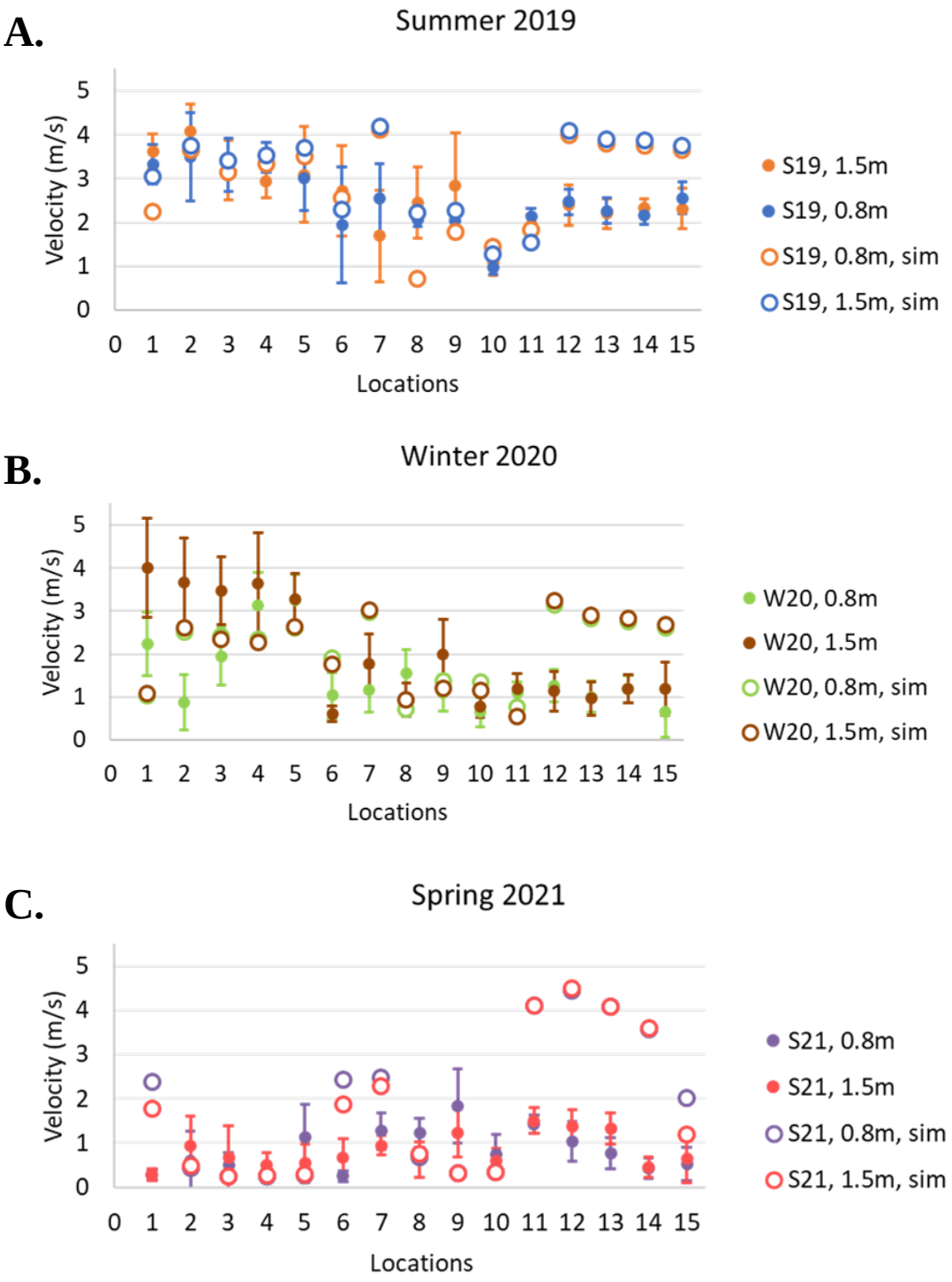

Figure 5.1 Comparison of experimental air velocity measurements (●) and simulated air velocity measurements (○) at heights of 0.8 m and 1.5 m in A. Summer 2019, B. Winter 2020, and C. Spring 2021.

5.4. Further works

This research investigated the overall trend and effect of three different environmental factors, temperature, relative humidity, and wind, on the microbiome diversity and antibiotic resistance in bacteria samples collected from a dairy farm across summer, winter, and spring. Examining the influence of each environmental factor on a single species of bacteria under carefully designed laboratory experiments could provide deeper insight into how and what type of antibiotic resistance is being promoted. Whole genome sequencing can be coupled with microbiome analysis to investigate the changes in ARG expressions to formulate a more direct relationship on how different environmental factors trigger specific species of bacteria. In this method, aerosolization and nebulization of bacteria into bioaerosols would also be taken into consideration. This could provide a deeper insight into exact mechanisms behind the development of ARGs in bacterial communities.

To more accurately simulate air flow around a building, or in this case a dairy barn, an effort can be made to develop a more complex and realistic 3D model of the facility that considers all or most of the present obstacles. Some obstacles such as the 400 cows can be simplified by using a porous media referred to as animal occupied zone (AOZ) to use the cow packing density instead of placing each individual simplified cow models throughout the barn. Heat generation from the cows can be accounted for using this method as well. This have been successfully studied and implemented in different studies on dairy cows (Doumbia et al., 2021; R. Mondaca and Y. Choi, 2016). This method can

be utilized to effectively and accurately model the effect of numerous cows without overloading the computational power and time required for the CFD simulations.

As was shown in the dissertation, both natural and mechanical ventilation have significant effects on the transmission of aerosols. Pathogenic and antibiotic resistant bacteria entrained in the air flow may be transported from contaminated spaces to clean areas and impact on surfaces. They can also be transported to the open environment and neighboring areas to be deposited on residential buildings or agricultural farms. Being airborne imposes mechanical stresses on bacteria and may trigger their defense mechanisms. Resuspension of bioaerosols in turbulent air flow may additionally affect their resistance against antibiotics, as was demonstrated in the Winter 2020 aerosol samples. Therefore, it is critical to optimize the air flow patterns and develop mitigation strategies in livestock facilities to reduce the spread of antibiotic resistant and potentially pathogenic bacteria. CFD models and simulations can be used to provide different layouts and mechanical or HVAC ventilation system designs to combat the spread of bioaerosols. Modifications to facilities could include installations of doors, walls, or air curtains to help mitigate the air flow direction to remove harmful particles and aerosolized bacteria from desired locations (Drewry et al., 2018; Saha et al., 2020; Viegas et al., 2020). Once the model has been verified and validated by comparing simulated results with experimental measurements, modifications to the design can be made to investigate effective mitigation strategies. It is often expensive and time-consuming to wait until the renovation has concluded or the proper equipment to be installed for investigation. One of the main advantages of utilizing CFD simulations would be that it provides detailed analysis and

prediction of air flow in different facilities to track and monitor the movement of bioaerosols to help determine how moderations to the building or ventilation systems can be made to improve the air quality in occupied places.

6. CONCLUSIONS

This study investigated the richness, diversity, and antibiotic resistance of bacterial communities in aerosol, manure, and lagoon samples collected in an open-stall dairy barn across three different seasons, Summer 2019, Winter 2020, and Spring 2021. Over 10,000 denoised sequence reads were generated from all samples that were used to identify and compare the bacterial taxonomy profiles among different samples, locations, and seasons. Firmicutes, Proteobacteria, Actinobacteriota, and Bacteroidota were shown to be the four most dominant phyla while *Bacillus*, *Acinetobacter*, *Sphingomonas*, and *Ruminococcaceae* UCG-005 were the four most dominant genera. Even though antibiotics were not administered to the dairy cows, strong antibiotic resistance was prevalent in manure samples and also displayed in aerosol samples consistently throughout three different seasons. Winter aerosol samples had the highest richness, lowest diversity, but strongest antibiotic resistance among the three seasons, demonstrating that lower temperature and higher relative humidity are correlated with stronger antibiotic resistance in aerosolized bacteria, despite low microbiome taxonomy abundance. Summer 2019 aerosol samples showed stronger antibiotic resistance compared to Spring 2021 aerosol samples. CFD simulations indicated that the southern and western sides of the dairy barn had the most turbulence in Summer 2019 and Winter 2020 as wind from the environment caused swirls as it entered the building. This was well correlated with strong antibiotic resistance patterns in aerosol samples from these sampling seasons. Spring 2021 had much weaker natural ventilation, but the microbiome diversity in aerosol and manure samples

were similar to each other, unlike Summer 2019 and Winter 2020 samples. This study demonstrates the critical importance and necessity of careful investigation of seasonal variables and air flow in dairy facilities, especially if they are open to the environment, to accurately monitor hotspots where antibiotic resistance can occur in the bacterial communities.

REFERENCES

Abraham, E. P., E. Chain, C. M. Fletcher, A. D. Gardner, N. G. Heatley, M. A. Jennings, and H. W. Florey. 1941. FURTHER OBSERVATIONS ON PENICILLIN. *The Lancet* 238(6155):177-189.

Adams, R. J., S. S. Kim, D. F. Mollenkopf, D. A. Mathys, G. M. Schuenemann, J. B. Daniels, and T. E. Wittum. 2018. Antimicrobial-resistant Enterobacteriaceae recovered from companion animal and livestock environments. *Zoonoses and Public Health* 65(5):519-527.

Ahmed, W., K. Richardson, J. P. S. Sidhu, P. Jagals, and S. Toze. 2014. Inactivation of faecal indicator bacteria in a roof-captured rainwater system under ambient meteorological conditions. *Journal of Applied Microbiology* 116(1):199-207.

Al-Nabulsi, A. A., T. M. Osaili, R. R. Shaker, A. N. Olaimat, Z. W. Jaradat, N. A. Zain Elabedeen, and R. A. Holley. 2015. Effects of osmotic pressure, acid, or cold stresses on antibiotic susceptibility of Listeria monocytogenes. *Food Microbiology* 46:154-160.

Alanis, A. J. 2005. Resistance to Antibiotics: Are We in the Post-Antibiotic Era? *Archives of Medical Research* 36(6):697-705.

Asheshov, E. H. 1966. Loss of antibiotic resistance in Staphylococcus aureus resulting from growth at high temperature. *Journal of general microbiology* 42(3):403-410.

Beck, S. H., A. Castillo, K. A. Kinney, A. Zuniga, Z. Mohammad, R. E. Lacey, and M. D. King. 2019. Monitoring of Pathogenic Bioaerosols in Beef Slaughter Facilities Based on Air Sampling and Airflow Modeling. *Applied Engineering in Agriculture* 35(6):1015-1036.

Billal, D. S., J. Feng, P. Leprohon, D. Légaré, and M. Ouellette. 2011. Whole genome analysis of linezolid resistance in Streptococcus pneumoniae reveals resistance and compensatory mutations. *BMC genomics* 12:512-512.

Blair, J. M. A., M. A. Webber, A. J. Baylay, D. O. Ogbolu, and L. J. V. Piddock. 2015. Molecular mechanisms of antibiotic resistance. *Nature Reviews Microbiology* 13(1):42-51.

Brągoszewska, E., and I. Biedroń. 2018. Indoor Air Quality and Potential Health Risk Impacts of Exposure to Antibiotic Resistant Bacteria in an Office Rooms in Southern Poland. *International Journal of Environmental Research and Public Health* 15(11).

Bray, J. R., and J. T. Curtis. 1957. An Ordination of the Upland Forest Communities of Southern Wisconsin. *Ecological Monographs* 27(4):325-349.

Burgos, J. M., B. A. Ellington, and M. F. Varela. 2005. Presence of Multidrug-Resistant Enteric Bacteria in Dairy Farm Topsoil. *Journal of Dairy Science* 88(4):1391-1398.

Burke, E. T. 1925. THE ARSENO-THERAPY OF SYPHILIS; STOVARSOL, AND TRYPARSAMIDE. *The British Journal of Venereal Diseases* 1(4):321.

Cadena, M., L. M. Durso, D. N. Miller, H. M. Waldrip, B. L. Castleberry, R. A. Drijber, and C. Wortmann. 2018. Tetracycline and Sulfonamide Antibiotic Resistance Genes in Soils From Nebraska Organic Farming Operations. *Frontiers in Microbiology* 9.

Callahan, B. J., P. J. McMurdie, and S. P. Holmes. 2017. Exact sequence variants should replace operational taxonomic units in marker-gene data analysis. *The ISME Journal* 11(12):2639-2643.

Callahan, B. J., P. J. McMurdie, M. J. Rosen, A. W. Han, A. J. A. Johnson, and S. P. Holmes. 2016. DADA2: High-resolution sample inference from Illumina amplicon data. *Nature Methods* 13(7):581-583.

Caporaso, J. G., J. Kuczynski, J. Stombaugh, K. Bittinger, F. D. Bushman, E. K. Costello, N. Fierer, A. G. Peña, J. K. Goodrich, J. I. Gordon, G. A. Huttley, S. T. Kelley, D. Knights, J. E. Koenig, R. E. Ley, C. A. Lozupone, D. McDonald, B. D. Muegge, M. Pirrung, J. Reeder, J. R. Sevinsky, P. J. Turnbaugh, W. A. Walters, J. Widmann, T. Yatsunenko, J. Zaneveld, and R. Knight. 2010. QIIME allows analysis of high-throughput community sequencing data. *Nature Methods* 7(5):335-336.

Claesson, M. J., Q. Wang, O. O'Sullivan, R. Greene-Diniz, J. R. Cole, R. P. Ross, and P. W. O'Toole. 2010. Comparison of two next-generation sequencing technologies for resolving highly complex microbiota composition using tandem variable 16S rRNA gene regions. *Nucleic acids research* 38(22):e200-e200.

CLSI.2014.Performance standards for antimicrobial susceptibility testing. Supplement M100-S24.

Cox, C. S., and C. M. Wathes. 1995. *Bioaerosols handbook*. Lewis Publishers.

Cummings, B., Y. Li, P. DeCarlo, M. Shiraiwa, and M. Waring. 2020. Indoor aerosol water content and phase state in U.S. residences: Impacts of relative humidity, aerosol mass and composition, and mechanical system operation. *Environmental Science: Processes & Impacts* 22.

Davies, J., and D. Davies. 2010. Origins and evolution of antibiotic resistance. *Microbiology and molecular biology reviews : MMBR* 74(3):417-433.

Diehl, D. L., and T. M. LaPara. 2010. Effect of Temperature on the Fate of Genes Encoding Tetracycline Resistance and the Integrase of Class 1 Integrons within Anaerobic and Aerobic Digesters Treating Municipal Wastewater Solids. *Environmental Science & Technology* 44(23):9128-9133.

Doumbia, E. M., D. Janke, Q. Yi, T. Amon, M. Kriegel, and S. Hempel. 2021. CFD modelling of an animal occupied zone using an anisotropic porous medium model with velocity depended resistance parameters. *Computers and Electronics in Agriculture* 181:105950.

Drewry, J. L., M. R. Mondaca, B. D. Luck, and C. Y. Choi. 2018. A Computational Fluid Dynamics Model of Biological Heat and Gas Generation in a Dairy Holding Area. *Transactions of the ASABE* 61(2):449-460.

Edelsberg, J., D. Weycker, R. Barron, X. Li, H. Wu, G. Oster, S. Badre, W. J. Langeberg, and D. J. Weber. 2014. Prevalence of antibiotic resistance in US hospitals. *Diagnostic Microbiology and Infectious Disease* 78(3):255-262.

Eliopoulos, G. M., and P. Huovinen. 2001. Resistance to Trimethoprim-Sulfamethoxazole. *Clinical Infectious Diseases* 32(11):1608-1614.

Faith, D. P. 1992. Conservation evaluation and phylogenetic diversity. *Biological Conservation* 61(1):1-10.

FDA. 2020. 2019 Summary Report On Antimicrobials Sold or Distributed for Use in Food-Producing Animals.

Fernstrom, A., and M. Goldblatt. 2013. Aerobiology and Its Role in the Transmission of Infectious Diseases. *Journal of Pathogens* 2013:493960.

Fossum, H. E., B. A. P. Reif, M. Tutkun, and T. Gjesdal. 2012. On the Use of Computational Fluid Dynamics to Investigate Aerosol Dispersion in an Industrial Environment: A Case Study. *Boundary-Layer Meteorology* 144(1):21-40.

Franke, J., and A. Baklanov. 2007. *Best Practice Guideline for the CFD Simulation of Flows in the Urban Environment: COST Action 732 Quality Assurance and Improvement of Microscale Meteorological Models*.

Gao, X.-L., M.-F. Shao, Q. Wang, L.-T. Wang, W.-Y. Fang, F. Ouyang, and J. Li. 2018. Airborne microbial communities in the atmospheric environment of urban hospitals in China. *Journal of Hazardous Materials* 349:10-17.

Ghafourian, S., N. Sadeghifard, S. Soheili, and Z. Sekawi. 2015. Extended Spectrum Beta-lactamases: Definition, Classification and Epidemiology. *Current Issues in Molecular Biology* 17(1).

Hall, M., and R. G. Beiko. 2018. 16S rRNA Gene Analysis with QIIME2. In *Microbiome Analysis: Methods and Protocols*, 113-129. R. G. Beiko, W. Hsiao, and J. Parkinson, eds. New York, NY: Springer New York.

Hassoun-Kheir, N., Y. Stabholz, J.-U. Kreft, R. de la Cruz, J. L. Romalde, J. Nesme, S. J. Sørensen, B. F. Smets, D. Graham, and M. Paul. 2020. Comparison of antibiotic-resistant bacteria and antibiotic resistance genes abundance in hospital and community wastewater: A systematic review. *Science of The Total Environment* 743:140804.

Hobday, R. A., and S. J. Dancer. 2013. Roles of sunlight and natural ventilation for controlling infection: historical and current perspectives. *Journal of Hospital Infection* 84(4):271-282.

Hoeksma, P., A. J. A. Aarnink, and N. W. M. Ogink. 2015. Effect of temperature and relative humidity on the survival of airborne bacteria = Effect van temperatuur en relatieve luchtvochtig-heid op de overleving van bacteriën in de lucht. Wageningen UR Livestock Research. Wageningen.

Hutchings, M. I., A. W. Truman, and B. Wilkinson. 2019. Antibiotics: past, present and future. *Current Opinion in Microbiology* 51:72-80.

Illumina. 2017. An introduction to Next-Generation Sequencing Technology.

Islam, M., S.-H. Kim, A. R. Son, S. C. Ramos, C.-D. Jeong, Z. Yu, S. H. Kang, Y.-I. Cho, S.-S. Lee, K.-K. Cho, and S.-S. Lee. 2021. Seasonal Influence on Rumen Microbiota, Rumen Fermentation, and Enteric Methane Emissions of Holstein and Jersey Steers under the Same Total Mixed Ration. *Animals* 11(4).

Janda, J. M., and S. L. Abbott. 2007. 16S rRNA gene sequencing for bacterial identification in the diagnostic laboratory: pluses, perils, and pitfalls. *Journal of clinical microbiology* 45(9):2761-2764.

Jehad, D., G. Hashim, A. Kadhim Zarzoor, and N. A. Che Sidik. 2015. Numerical Study of Turbulent Flow over Backward-Facing Step with Different Turbulence Models. *Journal of Advanced Research Design* 4:2289-7984.

Joshi, J. B., N. K. Nere, C. V. Rane, B. N. Murthy, C. S. Mathpati, A. W. Patwardhan, and V. V. Ranade. 2011. CFD simulation of stirred tanks: Comparison of turbulence models. Part I: Radial flow impellers. *The Canadian Journal of Chemical Engineering* 89(1):23-82.

Jung, J. H., J. E. Lee, and S. S. Kim. 2009. Thermal effects on bacterial bioaerosols in continuous air flow. *Science of The Total Environment* 407(16):4723-4730.

Kapoor, G., S. Saigal, and A. Elongavan. 2017. Action and resistance mechanisms of antibiotics: A guide for clinicians. *Journal of anaesthesiology, clinical pharmacology* 33(3):300-305.

Katoh, K., and D. M. Standley. 2013. MAFFT Multiple Sequence Alignment Software Version 7: Improvements in Performance and Usability. *Molecular Biology and Evolution* 30(4):772-780.

Kindrachuk, K. N., L. Fernández, M. Bains, and R. E. W. Hancock. 2011. Involvement of an ATP-dependent protease, PA0779/AsrA, in inducing heat shock in

response to tobramycin in Pseudomonas aeruginosa. *Antimicrobial agents and chemotherapy* 55(5):1874-1882.

Kirchhelle, C. 2018. Pharming animals: a global history of antibiotics in food production (1935–2017). *Palgrave Communications* 4(1):96.

Konopiński, M. K. 2020. Shannon diversity index: a call to replace the original Shannon's formula with unbiased estimator in the population genetics studies. *PeerJ* 8:e9391-e9391.

Kumar, A., and D. Pal. 2018. Antibiotic resistance and wastewater: Correlation, impact and critical human health challenges. *Journal of Environmental Chemical Engineering* 6(1):52-58.

Larsson, D. G. J. 2014. Antibiotics in the environment. *Upsala Journal of Medical Sciences* 119(2):108-112.

Launder, B. E., and D. B. Spalding. 1983. The numerical computation of turbulent flows. In *Numerical prediction of flow, heat transfer, turbulence and combustion*, 96-116. Elsevier.

Li, H., R. Li, H. Chen, J. Gao, Y. Wang, Y. Zhang, and Z. Qi. 2020a. Effect of different seasons (spring vs summer) on the microbiota diversity in the feces of dairy cows. *International Journal of Biometeorology* 64(3):345-354.

Li, J., J. Cao, Y.-g. Zhu, Q.-l. Chen, F. Shen, Y. Wu, S. Xu, H. Fan, G. Da, R.-j. Huang, J. Wang, A. L. de Jesus, L. Morawska, C. K. Chan, J. Peccia, and M. Yao. 2018. Global Survey of Antibiotic Resistance Genes in Air. *Environmental Science & Technology* 52(19):10975-10984.

Li, J., V. Narayanan, E. Kebreab, S. Dikmen, and J. G. Fadel. 2021. A mechanistic thermal balance model of dairy cattle. *Biosystems Engineering* 209:256-270.

Li, M. M., P. Ray, C. Teets, A. Pruden, K. Xia, and K. F. Knowlton. 2020b. Short communication: Increasing temperature and pH can facilitate reductions of cephapirin and antibiotic resistance genes in dairy manure slurries. *Journal of Dairy Science* 103(3):2877-2882.

Lin, H., J. Zhang, H. Chen, J. Wang, W. Sun, X. Zhang, Y. Yang, Q. Wang, and J. Ma. 2017. Effect of temperature on sulfonamide antibiotics degradation, and on antibiotic resistance determinants and hosts in animal manures. *Science of The Total Environment* 607-608:725-732.

Ling, A. L., N. R. Pace, M. T. Hernandez, and T. M. LaPara. 2013. Tetracycline Resistance and Class 1 Integron Genes Associated with Indoor and Outdoor Aerosols. *Environmental Science & Technology* 47(9):4046-4052.

Lozupone, C., and R. Knight. 2005. UniFrac: a New Phylogenetic Method for Comparing Microbial Communities. *Applied and Environmental Microbiology* 71(12):8228-8235.

Lundin, D., I. Severin, J. B. Logue, Ö. Östman, A. F. Andersson, and E. S. Lindström. 2012. Which sequencing depth is sufficient to describe patterns in bacterial α- and β-diversity? *Environmental Microbiology Reports* 4(3):367-372.

MacFadden, D. R., S. F. McGough, D. Fisman, M. Santillana, and J. S. Brownstein. 2018. Antibiotic resistance increases with local temperature. *Nature Climate Change* 8(6):510-514.

Maïzi, A., H. Dhaouadi, P. Bournot, and H. Mhiri. 2010. CFD prediction of odorous compound dispersion: Case study examining a full scale waste water treatment plant. *Biosystems Engineering* 106(1):68-78.

Mak, S., Y. Xu, and J. R. Nodwell. 2014. The expression of antibiotic resistance genes in antibiotic-producing bacteria. *Molecular Microbiology* 93(3):391-402.

Mardis, E. R. 2008. The impact of next-generation sequencing technology on genetics. *Trends in Genetics* 24(3):133-141.

Marthi, B., V. P. Fieland, M. Walter, and R. J. Seidler. 1990. Survival of bacteria during aerosolization. *Applied and Environmental Microbiology* 56(11):3463.

McEachran, A. D., B. R. Blackwell, J. D. Hanson, K. J. Wooten, G. D. Mayer, S. B. Cox, and P. N. Smith. 2015. Antibiotics, bacteria, and antibiotic resistance genes: aerial transport from cattle feed yards via particulate matter. *Environmental Health Perspectives* 123(4):337-343.

McFarland, A. R., J. S. Haglund, M. D. King, S. Hu, M. S. Phull, B. W. Moncla, and Y. Seo. 2010. Wetted Wall Cyclones for Bioaerosol Sampling. *Aerosol Science and Technology* 44(4):241-252.

Menter, F. 1993. Zonal Two Equation k-w Turbulence Models For Aerodynamic Flows. In *23rd Fluid Dynamics, Plasmadynamics, and Lasers Conference*. American Institute of Aeronautics and Astronautics.

Mirhoseini, S. H., M. Nikaeen, Z. Shamsizadeh, and H. Khanahmad. 2016. Hospital air: A potential route for transmission of infections caused by β-lactam–resistant bacteria. *American Journal of Infection Control* 44(8):898-904.

Mirskaya, E., and I. E. Agranovski. 2018. Sources and mechanisms of bioaerosol generation in occupational environments. *Critical Reviews in Microbiology* 44(6):739-758.

Munir, M., and I. Xagoraraki. 2011. Levels of Antibiotic Resistance Genes in Manure, Biosolids, and Fertilized Soil. *Journal of Environmental Quality* 40(1):248-255.

Nguyen, T. T., H. Wu, and N. Nishino. 2020. An investigation of seasonal variations in the microbiota of milk, feces, bedding, and airborne dust. *Asian-Australasian journal of animal sciences* 33(11):1858-1865.

Nicolaou, K. C., and S. Rigol. 2018. A brief history of antibiotics and select advances in their synthesis. *The Journal of Antibiotics* 71(2):153-184.

Nikoloudaki, O., W. J. F. Lemos Junior, L. Borruso, S. Campanaro, M. De Angelis, R. F. Vogel, R. Di Cagno, and M. Gobbetti. 2021. How multiple farming conditions correlate with the composition of the raw cow's milk lactic microbiome. *Environmental Microbiology* 23(3):1702-1716.

Noel, S. J., G. T. Attwood, J. Rakonjac, C. D. Moon, G. C. Waghorn, and P. H. Janssen. 2017. Seasonal changes in the digesta-adherent rumen bacterial communities of dairy cattle grazing pasture. *PLOS ONE* 12(3):e0173819.

Oliver, J. D. 2005. The viable but nonculturable state in bacteria. *Journal of microbiology* 43(spc1):93-100.

Otten, H. 1986. Domagk and the development of the sulphonamides. *Journal of Antimicrobial Chemotherapy* 17(6):689-690.

Pakari, A., and S. Ghani. 2021. Comparison of different mechanical ventilation systems for dairy cow barns: CFD simulations and field measurements. *Computers and Electronics in Agriculture* 186:106207.

Patankar, S. V., and D. B. Spalding. 1972. A calculation procedure for heat, mass and momentum transfer in three-dimensional parabolic flows. *International Journal of Heat and Mass Transfer* 15(10):1787-1806.

Pedregosa, F., G. Varoquaux, A. Gramfort, V. Michel, B. Thirion, O. Grisel, M. Blondel, P. Prettenhofer, R. Weiss, and V. Dubourg. 2011. Scikit-learn: Machine learning in Python. *the Journal of machine Learning research* 12:2825-2830.

Perry, R. H., D. W. Green, and J. O. Maloney. 1997. Perry's Chemical Engineers' Handbook (ed.). *Seventh, International edition*.

Poole, K. 2012. Bacterial stress responses as determinants of antimicrobial resistance. *Journal of Antimicrobial Chemotherapy* 67(9):2069-2089.

Price, M. N., P. S. Dehal, and A. P. Arkin. 2010. FastTree 2 – Approximately Maximum-Likelihood Trees for Large Alignments. *PLOS ONE* 5(3):e9490.

Pruesse, E., C. Quast, K. Knittel, B. M. Fuchs, W. Ludwig, J. Peplies, and F. O. Glöckner. 2007. SILVA: a comprehensive online resource for quality checked and aligned ribosomal RNA sequence data compatible with ARB. *Nucleic acids research* 35(21):7188-7196.

R. Mondaca, M., and C. Y. Choi. 2016. An Evaluation of Simplifying Assumptions in Dairy Cow Computational Fluid Dynamics Models. *Transactions of the ASABE* 59(6):1575-1584.

Ramirez, N., A. Afshari, and L. Norford. 2018. Validation of Simplified Urban-Canopy Aerodynamic Parametrizations Using a Numerical Simulation of an Actual Downtown Area. *Boundary-Layer Meteorology* 168(1):155-187.

Ramponi, R., and B. Blocken. 2012. CFD simulation of cross-ventilation for a generic isolated building: Impact of computational parameters. *Building and Environment* 53:34-48.

Richards, P. J., and R. P. Hoxey. 1993. Appropriate boundary conditions for computational wind engineering models using the k-ϵ turbulence model. *Journal of Wind Engineering and Industrial Aerodynamics* 46-47:145-153.

Rodloff, A. C., E. J. C. Goldstein, and A. Torres. 2006. Two decades of imipenem therapy. *Journal of Antimicrobial Chemotherapy* 58(5):916-929.

Rojano, F., P.-E. Bournet, M. Hassouna, P. Robin, M. Kacira, and C. Y. Choi. 2019. Modelling the impact of air discharges caused by natural ventilation in a poultry house. *Biosystems Engineering* 180:168-181.

Saha, C. K., Q. Yi, D. Janke, S. Hempel, B. Amon, and T. Amon. 2020. Opening Size Effects on Airflow Pattern and Airflow Rate of a Naturally Ventilated Dairy Building—A CFD Study. *Applied Sciences* 10(17).

Sanger, F., S. Nicklen, and A. R. Coulson. 1977. DNA sequencing with chain-terminating inhibitors. *Proceedings of the National Academy of Sciences* 74(12):5463-5467.

Shannon, C. E. 1948. A mathematical theory of communication. *The Bell System Technical Journal* 27(3):379-423.

Shih, T.-H., W. W. Liou, A. Shabbir, Z. Yang, and J. Zhu. 1995. A new k-ϵ eddy viscosity model for high reynolds number turbulent flows. *Computers & Fluids* 24(3):227-238.

Sosnowski, M., J. Krzywanski, and R. Gnatowska. 2017. Polyhedral meshing as an innovative approach to computational domain discretization of a cyclone in a fluidized bed CLC unit. *E3S Web Conf.* 14.

Sun, W., X. Qian, J. Gu, X.-J. Wang, and M.-L. Duan. 2016. Mechanism and Effect of Temperature on Variations in Antibiotic Resistance Genes during Anaerobic Digestion of Dairy Manure. *Scientific Reports* 6(1):30237.

Tamber, S., and R. Hancock. 2003. On the mechanism of solute uptake in Pseudomonas. *Frontiers in bioscience : a journal and virtual library* 8:s472-483.

Tan, H., M. Cai, Q. Fan, L. Liu, F. Li, P. W. Chan, X. Deng, and D. Wu. 2017. An analysis of aerosol liquid water content and related impact factors in Pearl River Delta. *Science of The Total Environment* 579:1822-1830.

Tang, J. W. 2009. The effect of environmental parameters on the survival of airborne infectious agents. *Journal of the Royal Society, Interface* 6 Suppl 6(Suppl 6):S737-S746.

Tenover, F. C. 2006. Mechanisms of Antimicrobial Resistance in Bacteria. *The American Journal of Medicine* 119(6, Supplement 1):S3-S10.

Tomasello, N., F. Valenti, G. Cascone, and S. M. C. Porto. 2019. Development of a CFD Model to Simulate Natural Ventilation in a Semi-Open Free-Stall Barn for Dairy Cows. *Buildings* 9(8).

Tominaga, Y., A. Mochida, R. Yoshie, H. Kataoka, T. Nozu, M. Yoshikawa, and T. Shirasawa. 2008. AIJ guidelines for practical applications of CFD to pedestrian wind environment around buildings. *Journal of Wind Engineering and Industrial Aerodynamics* 96(10):1749-1761.

Tong, Y., and B. Lighthart. 1997. Solar Radiation Is Shown to Select for Pigmented Bacteria in the Ambient Outdoor Atmosphere. *Photochemistry and Photobiology* 65(1):103-106.

Uddin, M. J., and J. Ahn. 2018. Characterization of β-lactamase- and efflux pump-mediated multiple antibiotic resistance in Salmonella Typhimurium. *Food Science and Biotechnology* 27(3):921-928.

Viegas, J., P. Kaluzny, A. Durand, L. Fluchaire, D. Franco, C. Saldanha, J. Morais, P. Morais, L. Carrasco, and L. Pinto. 2020. Full-size experimental assessment of the aerodynamic sealing of air curtains for particulate matter. *Building Services Engineering Research and Technology* 42:014362442097640.

Wang, H., H. Wang, F. Gao, P. Zhou, and Z. Zhai. 2018. Literature review on pressure–velocity decoupling algorithms applied to built-environment CFD simulation. *Building and Environment* 143:671-678.

Wang, H., and Z. Zhai. 2016. Advances in building simulation and computational techniques: A review between 1987 and 2014. *Energy and Buildings* 128:319-335.

Wepking, C., B. Avera, B. Badgley, J. E. Barrett, J. Franklin, K. F. Knowlton, P. P. Ray, C. Smitherman, and M. S. Strickland. 2017. Exposure to dairy manure leads to greater antibiotic resistance and increased mass-specific respiration in soil microbial

communities. *Proceedings of the Royal Society B: Biological Sciences* 284(1851):20162233.

Whittaker, R. H. 1960. Vegetation of the Siskiyou Mountains, Oregon and California. *Ecological Monographs* 30(3):279-338.

Wichmann, F., N. Udikovic-Kolic, S. Andrew, and J. Handelsman. 2014. Diverse Antibiotic Resistance Genes in Dairy Cow Manure. *mBio* 5(2):e01017-01013.

Williams, D. H. 1996. The glycopeptide story – how to kill the deadly 'superbugs'. *Natural Product Reports* 13(6):469-477.

Windels, E. M., J. E. Michiels, M. Fauvart, T. Wenseleers, B. Van den Bergh, and J. Michiels. 2019. Bacterial persistence promotes the evolution of antibiotic resistance by increasing survival and mutation rates. *The ISME Journal* 13(5):1239-1251.

Wu, H., Q. D. Nguyen, T. T. M. Tran, M. T. Tang, T. Tsuruta, and N. Nishino. 2019. Rumen fluid, feces, milk, water, feed, airborne dust, and bedding microbiota in dairy farms managed by automatic milking systems. *Animal Science Journal* 90(3):445-452.

Wu, W., J. Zhai, G. Zhang, and P. V. Nielsen. 2012. Evaluation of methods for determining air exchange rate in a naturally ventilated dairy cattle building with large openings using computational fluid dynamics (CFD). *Atmospheric Environment* 63:179-188.

Yoneyama, H., and R. Katsumata. 2006. Antibiotic Resistance in Bacteria and Its Future for Novel Antibiotic Development. *Bioscience, Biotechnology, and Biochemistry* 70(5):1060-1075.

Zaman, S. B., M. A. Hussain, R. Nye, V. Mehta, K. T. Mamun, and N. Hossain. 2017. A Review on Antibiotic Resistance: Alarm Bells are Ringing. *Cureus* 9(6):e1403-e1403.

Zhai, Z. J., Z. Zhang, W. Zhang, and Q. Y. Chen. 2007. Evaluation of Various Turbulence Models in Predicting Airflow and Turbulence in Enclosed Environments by CFD: Part 1—Summary of Prevalent Turbulence Models. *HVAC&R Research* 13(6):853-870.

Zhang, T., Y. Yang, and A. Pruden. 2015. Effect of temperature on removal of antibiotic resistance genes by anaerobic digestion of activated sludge revealed by metagenomic approach. *Applied Microbiology and Biotechnology* 99(18):7771-7779.

Zhao, Y., A. J. A. Aarnink, R. Dijkman, T. Fabri, M. C. M. de Jong, and P. W. G. Groot Koerkamp. 2012. Effects of temperature, relative humidity, absolute humidity, and evaporation potential on survival of airborne Gumboro vaccine virus. *Applied and Environmental Microbiology* 78(4):1048-1054.

Zheng, W., J. Huyan, Z. Tian, Y. Zhang, and X. Wen. 2020. Clinical class 1 integron-integrase gene – A promising indicator to monitor the abundance and elimination of antibiotic resistance genes in an urban wastewater treatment plant. *Environment International* 135:105372.

Zhou, C., Y. Yujun, and A. Y. Jong. 1990. Mini-prep in ten minutes. *Biotechniques* 8(2):2.

APPENDIX

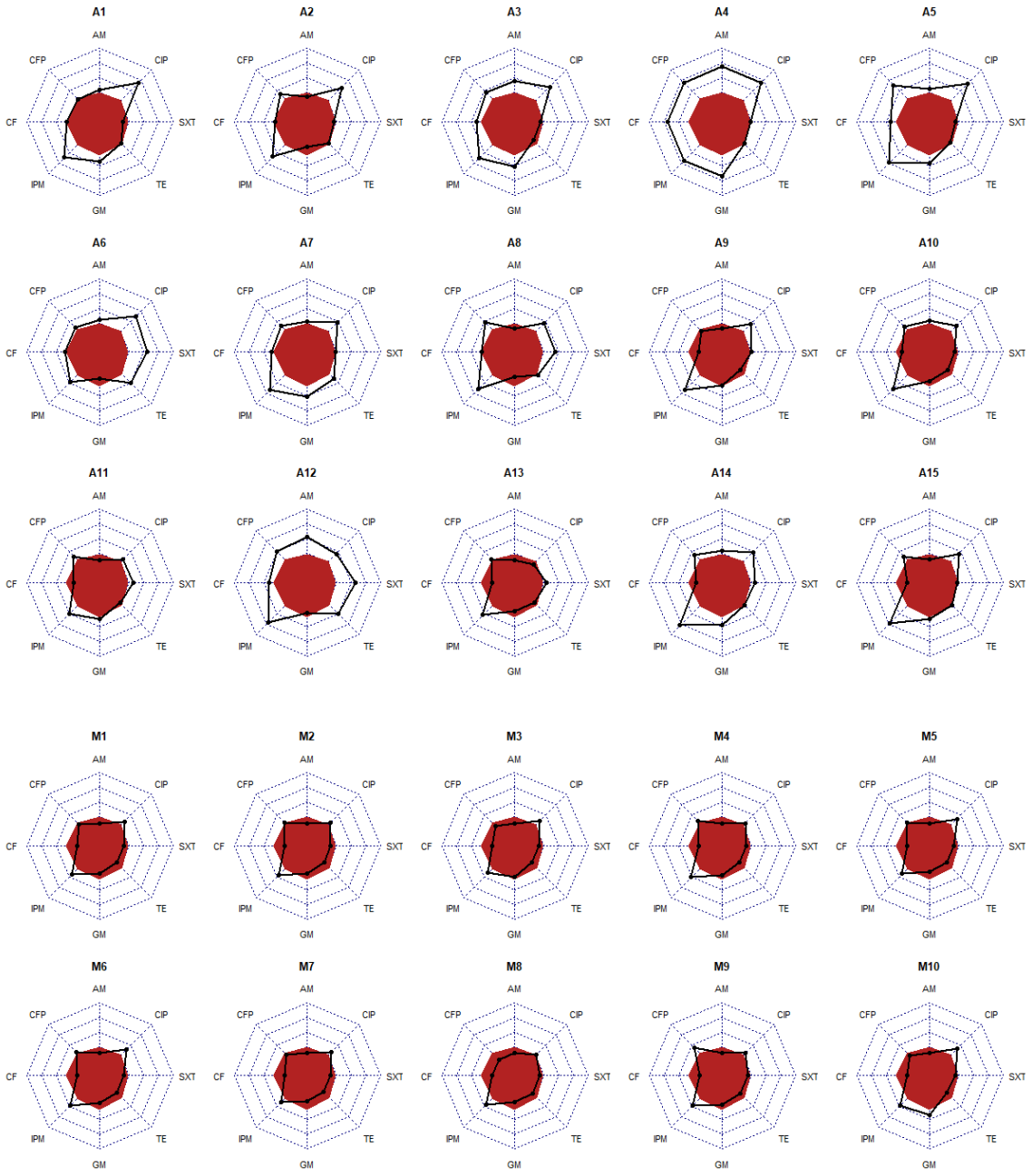

Figure 6.1 Antibiotic resistance shown in radar charts for aerosol and manure samples in Summer 2019. Red zone indicates resistance zone of inhibition for the eight antibiotics and black lines show zone of inhibition of each sample to each antibiotic.

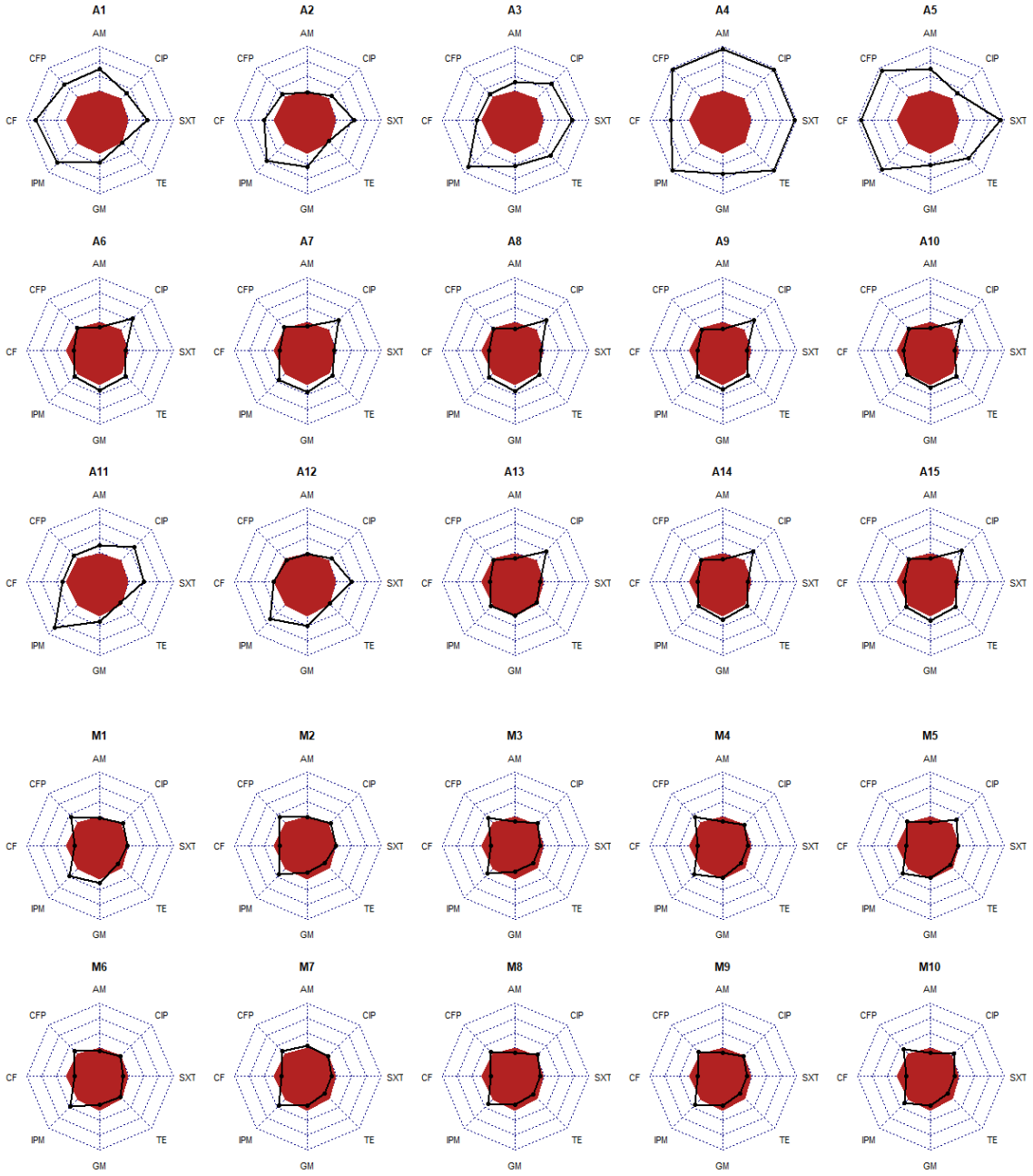

Figure 6.2 Antibiotic resistance shown in radar charts for aerosol and manure samples in Winter 2020. Red zone indicates resistance zone of inhibition for the eight antibiotics and black lines show zone of inhibition of each sample to each antibiotic.

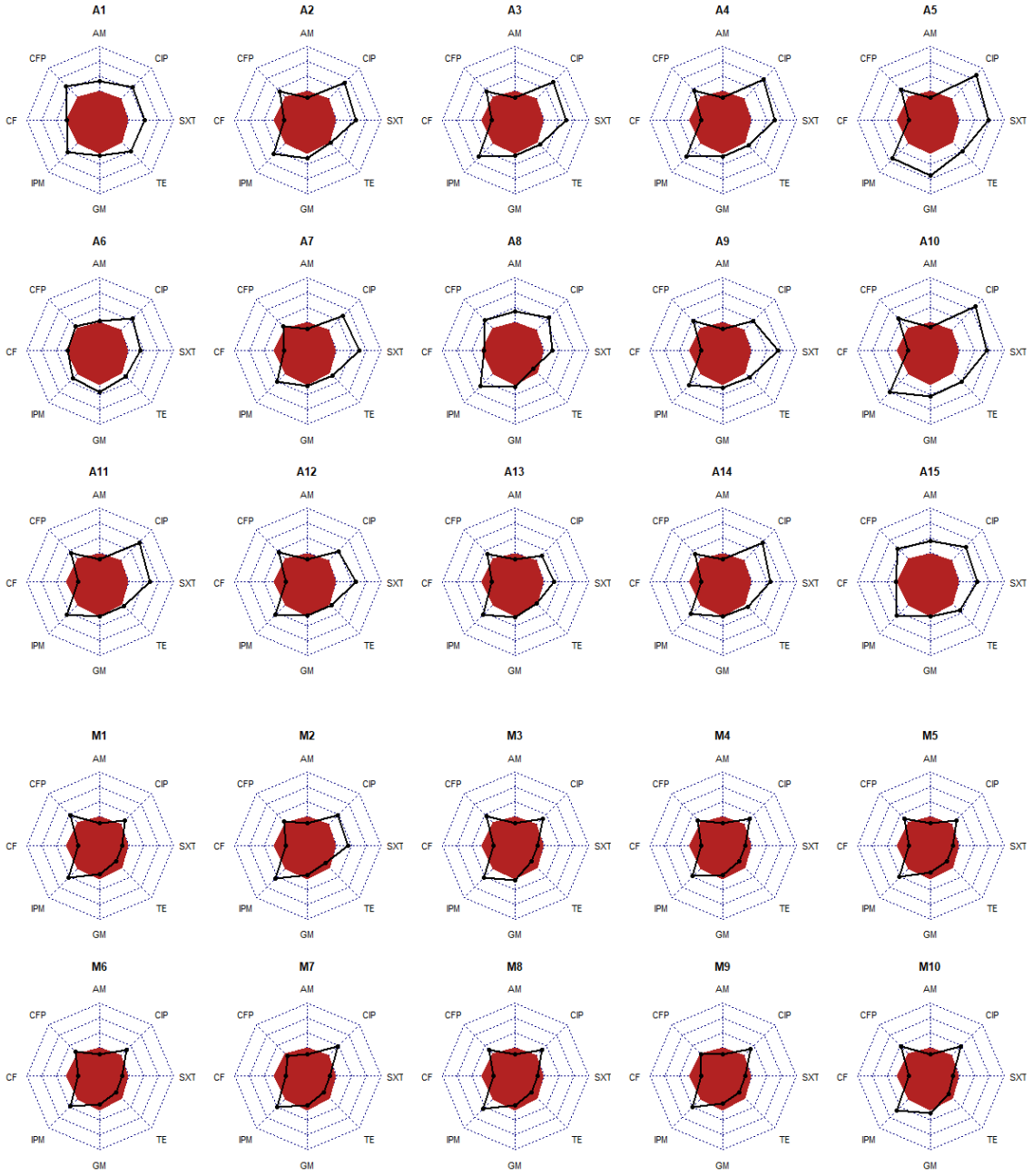

Figure 6.3 Antibiotic resistance shown in radar charts for aerosol and manure samples in Spring 2021. Red zone indicates resistance zone of inhibition for the eight antibiotics and black lines show zone of inhibition of each sample to each antibiotic.